Available online at www.sciencedirect.com

SCIENCE DIRECT®

Developmental Biology 275 (2004) 104–123

DEVELOPMENTAL BIOLOGY

www.elsevier.com/locate/ydbio

The orphan COUP-TF nuclear receptors are markers for neurogenesis from cnidarians to vertebrates

Dominique Gauchat[a,1], Hector Escriva[b], Marijana Miljkovic-Licina[a], Simona Chera[a], Marie-Claire Langlois[c], Agnès Begue[b], Vincent Laudet[b,c], Brigitte Galliot[a,*]

[a]*Department of Zoology and Animal Biology, University of Geneva, Sciences III, CH-1211 Geneva 4, Switzerland*
[b]*UMR 49 du CNRS, Ecole Normale Supérieure de Lyon, F-69364 Lyon Cedex 07, France*
[c]*UMR 319 du CNRS, Institut de Biologie de Lille, Institut Pasteur, F-59019 Lille Cedex, France*

Received for publication 13 May 2003, revised 2 July 2004, accepted 8 July 2004
Available online 8 September 2004

Abstract

In bilaterians, COUP-TF nuclear receptors participate in neurogenesis and/or CNS patterning. In hydra, the nervous system is formed of sensory mechanoreceptor cells (nematocytes) and neuronal cells, both lineages deriving from a common stem cell. The hydra *COUP-TF* gene, *hyCOUP-TF*, which encodes highly conserved DNA-binding and ligand-binding domains, belongs to the monophyletic COUP-TFs orphan receptor family (NR2F). In adult polyps, *hyCOUP-TF* is expressed in nematoblasts and a subset of neuronal cells. Comparative BrDU labeling analyses performed on cells expressing either *hyCOUP-TF* or the paired-like gene *prdl-b* showed that *prdl-b* expression corresponded to early stages of proliferation, while *hyCOUP-TF* was detected slightly later. *HyCOUP-TF* and *prdl-b* expressing cells disappeared in sf-1 mutants becoming "nerve-free". Moreover *hyCOUP-TF* and *prdl-b* expression was excluded from regions undergoing developmental processes. These data suggest that *hyCOUP-TF* and *prdl-b* belong to a genetic network that appeared together with neurogenesis during early metazoan evolution. The hyCOUP-TF protein specifically bound onto the evolutionarily conserved DR1 and DR5 response elements, and repressed transactivation induced by RAR:RXR nuclear receptors in a dose-dependent manner when expressed in mammalian cells. Hence, a cnidarian transcription factor can be active in vertebrate cells, implying that functional interactions between COUP-TF and other nuclear receptors were evolutionarily conserved.

Keywords: Hydra; Cnidaria; Orphan nuclear receptors; COUP-TF; Paired-like homeobox gene; Transactivation; Mechanoreceptor cells; Nematocytes; Neurogenesis; Stem cells; Evolution; BrdU labeling

Introduction

Hydra is a freshwater bilayered animal, organized as a tube with at one extremity, a single opening surrounded by a ring of tentacles, defining the head region, and at the other, a basal disc used by the animal to attach to the substrate. Hydra belongs to the Cnidaria, which together with Ctenophora are the first metazoan phyla in the animal kingdom to differentiate highly specialized cell types such as myoepithelial cells, nematocytes, and neurons. The emergence of active movements and feeding behavior, which relies on the presence of a nervous system, is a major hallmark of metazoan organization. Therefore, hydra represents an excellent model to study molecular mechanisms implicated in the early differentiation of nervous systems in animal evolution. Moreover, cnidarians also provide a model system for developmental biology, since they display an oral-aboral patterning process, a process easily amenable to experimentation during budding, regeneration, transplantation, and reaggregation (Holstein et al., 2003).

* Corresponding author. Department of Zoology and Animal Biology, University of Geneva, Sciences III, 30 Quai Ernest Ansermet, CH-1211 Geneva 4, Switzerland. Fax: +41 22 379 67 95.
E-mail address: brigitte.galliot@zoo.unige.ch (B. Galliot).
[1] Present address: Université de Montréal, Département de Microbiologie et d'Immunologie, Faculté de Médecine, Montréal, Quebec, Canada H3T 1J4.

0012-1606/$ - see front matter © 2004 Elsevier Inc. All rigths reserved.
doi:10.1016/j.ydbio.2004.07.037

In cnidarians, active behaviors rely on a simple nervous system, composed of nerve cells, either sensory or ganglia, and nematocytes, which are mechanoreceptor cells, specific to the Cnidaria phylum. In hydra, nematocytes are abundant, representing 35% of all cell types (David, 1973), particularly in tentacles where they are responsible for the food capture (Tardent, 1995). The cnidocil apparatus of nematocytes displays similarities with cnidocils present in sensory cells of nematodes, insects, and vertebrates and might thus represent a progenitor of metazoan mechanoreceptors (Holstein and Hausmann, 1988; Holtmann and Thurm, 2001b). Upon stimulation of their cnidocil by a prey, nematocytes discharge a highly osmotically pressured capsule named nematocyst that contains anions and toxins. This discharge process occurs in few milliseconds (Holstein and Tardent, 1984) and can function independently of the nervous system (Aerne et al., 1991). Thus, nematocytes can be considered as autonomous receptor–effector units, even though synaptic connections to nerve cells were demonstrated ultrastructurally (Westfall, 1996; Westfall et al., 2002) and shown to regulate their activity (Holtmann and Thurm, 2001a; Kass-Simon and Scappaticci, 2002). The neuronal and nematocyte cell lineages derive from a common stem cell, a pluripotent interstitial cell, which can also differentiate towards the gland cell lineage and the gametes (Bode, 1996). In hydra, precursor cells to nerve cells are blocked in G2 and, upon appropriate signaling, undergo a limited number of mitotic events that will provide mature nerve cells (Schaller et al., 1989). In contrast, precursors to nematocytes (nematoblasts), which are in the ectodermal layer along the body column, undergo a variable number of synchronous divisions, from 3 to 5, forming nests of cells communicating by cytoplasmic bridges, before differentiating the nematocyst, a sophisticated Golgi-derived intracellular structure (Lehn, 1951; Rich and Tardent, 1969; Tardent, 1995). Nematocysts can be of four different types, stenoteles, desmonemes, holotrichous, and atrichous isorhiza (see in Holstein and Emschermann, 1995), according to a body axis position-dependent differentiation process (Fujisawa et al., 1986). Once harboring mature capsules, most nematocytes will migrate towards the tentacles according to a guiding process (Campbell and Marcum, 1980; Weber et al., 1978).

The underlying genetic mechanisms responsible for the emergence of mechanoreceptor and neuronal cell types along evolution are still poorly understood (Anderson, 1990; Mackie, 1990); however, the cnidarian version of a dozen genes known to regulate neurogenesis in bilaterian species was characterized within the last 10 years. Among those, four gene families were shown to be expressed in the nematocyte lineage in hydra: *CnASH*, the *Achaete-scute* homolog (Grens et al., 1995), *prdl-b*, a paired-like homeogene (Gauchat et al., 1998), *hyzic*, a Zic homolog (Lindgens et al., 2004), and *hyDkk3*, the Dickkopf-3 homolog (Fedders et al., 2004).

In this paper, we focused on the cellular and developmental regulation of the hydra *COUP-TF* homolog gene (Escriva et al., 1997) and used the *prdl-b* gene for comparative cell analyses. *COUP-TFs* genes bring a major contribution to neurogenesis and neurophysiology in vertebrates (Cooney et al., 2001; Pereira et al., 2000) and also affect the development of nervous system in *Drosophila* (Mlodzik et al., 1990) and amphioxus (Langlois et al., 2000). Nuclear receptors (NRs) are ligand-dependent transcription factors, activated by steroid hormones, and non-steroid molecules such as retinoic acid, thyroid hormone and vitamin D (Moras and Gronemeyer, 1998). However, no cognate ligand was identified for the COUP-TFs and EAR-2 NR, which are therefore considered as "orphan" NR (Giguere, 1999). Together with the HNF4 (NR2A), RXR (NR2B), TR2/4 (NR2C), DHR78 (NR2D), and TLL (NR2E) NRs, COUP-TFs (NR2F) define the class II of the NR superfamily (Nuclear Receptor Nomenclature Committee, 1999). *COUP-TF* homologs were identified in a wide range of metazoans from cnidarians to protostomes and deuterostomes (Devine et al., 2002; Escriva et al., 1997; Grasso et al., 2001; Langlois et al., 2000), showing an extensive degree of sequence identity in the DNA-binding domain (C domain) and the ligand-binding domain (E domain). In cnidarians, a *COUP-TF* gene was detected in hydra, *RXR* and *FTZ-F1* genes in the *Anemonia sulcata* (Escriva et al., 1997), a *RXR* homolog was characterized in the jellyfish *Tripedalia cystophora* (Kostrouch et al., 1998) and more recently, six distinct NR genes with clearly identifiable DNA-binding and ligand-binding domains were isolated in the coral *Acropora millipora* (Grasso et al., 2001), four of them being assessed to the class II NR. These results demonstrate that *COUP-TF* and *RXR* genes appeared very early during metazoan evolution, before the divergence between Cnidaria and Bilateria. Moreover, their high degree of conservation in the functional domains implies that they support essential functions among all metazoans. In this paper, we show that *hyCOUP-TF* like the paired-like gene *prdl-b* is expressed in both, nematocyte and neuronal cell lineages, as well as in a subset of interstitial stem cells. In the temperature-sensitive sf-1 mutant that eliminates its interstitial cell lineage at non-permissive temperature *hyCOUP-TF* and *prdl-b*-expressing cells disappear. In addition measurements of the BrdU labeling indexes in *hyCOUP-TF* and *prdl-b* expressing cells clearly show that both genes are induced at early stages of the nematocyte pathway, although with different kinetics and distinct regulations along this pathway. Finally, when expressed in mammalian cells, hyCOUP-TF is able to repress transactivation of reporter constructs induced by RAR:RXR NR.

Material and methods

Hydra culture, regeneration experiments and production of "nerve-free" animals

Hydra vulgaris (*Hv*) from the Zürich (gift of S. Hoffmeister) and Holland (gift from D. Campbell) strains,

Hydra magnipapillata (*Hm*) from the Hm 105 and sf-1 strains (gift from T. Holstein) or *Hydra vulgaris* from the AEP strain (gift from T. Bosch) were cultured in hydra medium (HM: 1 mM NaCl, 1 mM $CaCl_2$, 0.1 mM KCl, 0.1 mM $MgSO_4$, 1 mM Tris pH 7.6) and fed 5 days a week with hatched *Artemia nauplii*. After a 2-day starvation period, regeneration experiments were performed at 19°C on budless hydra, bisected at mid-gastric position. Sexual hydra were either collected among the *Hv* Holland strain or obtained from the *Hv* AEP strain after induction (Martin et al., 1997). To obtain "nerve-free" hydra, sf-1 hydra were induced at 26°C for 2 days (Marcum et al., 1980).

Isolation of hyCOUP-TF cDNAs

A 117-bp PCR fragment corresponding to the *hyCOUP-TF* gene (Escriva et al., 1997) was used as a probe to screen a lambda-gt11 *Hv* cDNA library (gift from C. Schaller). A single clone, named cDNA type I, 981 bp long, was isolated out of 10^6 phages. The region of this clone encompassing the C and D domains was used to screen a second cDNA library prepared from adult hydra polyps (gift from H. Bode). Hybridization were performed overnight at 37°C in 40% formamide, 7× SSC, 5× Denhardt's solution, 0.5% SDS, 0.1 mg/ml denatured salmon sperm DNA. Membranes were washed twice in 2× SSC, then 0.1× SSC at 37°C for 15 min. The inserts were subcloned in BlueScript vectors and sequenced on both strands.

Phylogenetic analysis of the hydra COUP sequences

NR sequences related to the deduced hyCOUP-TF protein were collected on databases using the Blast search on the Expasy server (www.expasy.org). 51 representative sequences were selected and aligned (see supplement 4) using ClustalW at the Pole Bioinformatique Lyonnais (http://pbil.univ-lyon1.fr) and the Genetic Data Environment 2.2 software (Larsen et al., 1993). Sequences and alignments can be found on Nurebase: http://ens-lyon/LBMC/laudet/nurebase.html (Duarte et al., 2002). Phylogenetic analyses were performed on sequences corresponding either to the C–F domains (318 residues after pairwise gap removal), or only the C domain (60 residues) following the procedure previously described (Galliot et al., 1999).

Human-hydra hybrid constructs

The hyCOUP-chim1 clone was constructed by the "overlap extension" mutagenesis technique (Yon and Fried, 1989) using the hyCOUP-TF type I and type III cDNAs as templates and adding 25 residues (MQQHIECVVCGDK-SSGKHYGQFTCE) from the evolutionarily conserved N-terminus of the huCOUP-TF1 C domain to the hyCOUP-TF N-terminus. Three consecutive PCRs were performed using the following primers: 5C-hu; attatgcagcagcacatcgagtgcgtg, 3C-hu: tcgtctaatgcttcgcttgaagaaactttt, 5D-hy: ctagaaggttc-tatggttgatcag, 5C-chim: aaaagtttcttcaagcgaagcattagacga, 3D-hy: tgtaatccattataatggctg, 3tot-hy: cattgtatcacctaagaggag. PCR1 amplified 3 distinct templates: huCOUP-TF1 (5C-hu, 3C-hu primers), hyCOUP-TF type I (5C-hy, 3D-hy primers) and hyCOUP-TF type III (5D-hy, 3tot-hy primers). PCR2 was performed on 200 ng of the previously amplified and annealed hyCOUP-TF type I and type III fragments, and provided the full hyCOUP-TF1 (5C-hy, 3tot-hy primers). Finally, PCR3 was performed on 200 ng of the previously amplified huCOUP-TF1 (PCR1) and full hyCOUP-TF (PCR2) fragments using the 5C-hu and 3tot-hy primers. Profiles of PCR1, PCR2 and PCR3 were identical (94°C 10 min, [94°C 30 s, 45°C 30 s, 72° 3 min] ×5, [94°C 30 s, 45°C 30 s, 72° 1 min] ×20, 72°C 7 min). The PCR3 amplification product (hyCOUP-chim1, 1438 bp) was cloned into the pCR-TOPO vector (Invitrogen) and sequenced. The hyCOUP-chim2 clone was constructed similarly by adding to the 5′ end of hyCOUP-chim1 the region corresponding to the A/B domain of huCOUP-TF (84 residues). The GC-rich 271 bp fragment encompassing the huCOUP-TF1 5′ end was first amplified with the huCOUP-for1 (tagattatggcaatggtagttagcagc) and huCOUP-rev2 (ccccgcaccacgcactcgatgtgctgctg) primers using the Advantage GC cDNA polymerase mix (Clontech) 1/5 (94°C 5 min, [94°C 30 s, 49°C 1 min, 72°C 1 min] 30×, 72°C 10 min). The hyCOUP-chim1 fragment was amplified with the COUP-chim1.1 (cagcagcacatcgagtgcgtg) and COUP-chim1.2 (cattgtatcacctaagaggaggc) primers using the Qiagen Taq polymerase (94°C 5 min, [94°C 30 s, 53°C 1 min, 72°C 2 min] 30×, 72°C 10 min). Both fragments were purified from gel, mixed, purified again (ROCHE, High Pure PCR Product Purification Kit) and then annealed in the absence of any primers but in the presence of Advantage GC cDNA polymerase mix, Taq polymerase (50X Taq mix used 1×), dNTP (0.2 mM each), GC cDNA PCR reaction buffer for 15 min at 45°C after denaturation (94°C 5 min) following a slow temperature downshift (1°C per min). The huCOUP-for2 (cccatagatatgg-caatggtagttagcagc) and COUP-chim1.2 primers were subsequently added and the 1710 bp hybrid product was amplified (94°C 5 min, [94°C 30 s, 53°C 1 min, 72°C 2 min] 30×, 72°C 10 min). After reamplification, the hyCOUP-chim2 PCR product was first sub-cloned into the pDrive vector (Quiagen), digested *Bam*HI/*Sal*I and then inserted into the pSG5 vector at the *Bam*HI site for eukaryotic expression.

In situ hybridization (ISH)

Standard in situ hybridization was performed on whole mount animals, following the procedures described in (Grens et al., 1996). The digoxigenin (DIG)-labeled *hyCOUP-TF* riboprobe was prepared after *Pst*I digestion of the hyCOUP-TF type I cDNA (800 bp); the DIG-labeled *prdl-b* riboprobe, after *Nsi*I digestion of the *prdl-b* cDNA (clone 33, 700 bp). After NBT-BCIP staining, animals were

stained with DAPI (0.01 μg/ml in PBS) for 2 to 5 min at RT, then washed 2× 5 min in PBS and once in water. Samples were mounted in DABCO (Sigma) and nests were counted on a Zeiss Axioplan2 microscope. For cell-type determination, 10 μm cryosections were performed after NBT/BCIP or Fast Red staining.

Double-labeling in situ hybridization was carried out in the InSituPro robot (INTAVIS Bioanalytical Instruments AG) as previously mentioned with following modifications: Animals were incubated in hybridization solution (50% formamide, 5× SSC, 0.1% Tween 20, 0.1% CHAPS, 1× Denhardt's solution, 0.01% heparine, 0.02% tRNA in DEPC H_2O) containing 1 to 2 μg/ml DIG-labeled *prdl-b* RNA probe and a fluorescein-labeled *COUP* RNA probe for 16 h at 55°C. For detection, samples were incubated with two antibodies simultaneously, the sheep anti-DIG Fab fragments coupled to alkaline phosphatase (1:2000, Roche) and the sheep anti-fluorescein Fab fragments coupled to horseradish peroxidase (1:100, Roche) during 6 h at RT in the robot. Unbound antibodies were removed by numerous washes in MAB (100 mM maleic acid, 150 mM Tris HCl, pH 7.5): 4× 12 min, 4× 30 min, 4× 1 h, 2× 2 h. Animals were then washed in TNT buffer (150 mM NaCl, 100 mM Tris HCl, pH7.5, 0.05% Tween-20) 3 × 5 min and incubated in biotinyl–tyramide mix diluted in the amplification buffer (1:50, PerkinElmer Life Sciences) for 30 min at RT, before being washed again in TNT buffer 3× 5 min. Alexa-488-conjugated streptavidin antibody (1:100, Molecular Probes) was added in the amplification buffer and incubation was carried out at RT for 30 min. Animals were subsequently washed in TNT buffer 3× 5 min and stained with Fast Red (DAKO Cytomation) for 15–90 min at RT in the dark. Staining was stopped by washing in TNT buffer 3× 5 min at RT. Samples were mounted as above and screened for fluorescent signals on a Zeiss Axioplan2 microscope equipped with the FITC, rhodamine, and DAPI filters.

BromodeoxyUridine (BrdU) labeling

Hydra were starved for 1 day and then exposed to 5 mM BrdU (Sigma) for variable periods of time as indicated. Animals were then fixed in PFA 4% and processed for in situ hybridization. After riboprobe detection, animals were washed in PBST (PBS, 0.1% Triton X100) 3× 5 min, treated with 2N HCl for DNA denaturation for 40 min at RT, washed in PBST at least 5× over 15 min and then incubated with the anti-BrdU antibody (1:20, BrdU labeling and detection Kit I Roche) for 1 h at 37°C. After three washes in PBS animals were incubated for 3 h at RT with the anti-mouse Alexa Fluor 488 antibody (1:500, Molecular Probes), washed again in PBS, mounted in Mowiol and screened for fluorescence as given above. Counting of nests displaying BrdU labeled nuclei was performed with the 100× objective on 40 to 100 nests per animal expressing either *hyCOUP-TF* or *prdl-b* and a minimum of five animals was counted for each condition.

Gel retardation assays

The hyCOUP-chim1, hyCOUP-chim2, and amphiCOUP plasmids were used to produce the corresponding proteins in reticulocyte lysate according to the supplier procedure (TnT kit, Promega). The double-stranded oligonucleotides DR1: cgcgatttgaggtcaaaggtcacac-agtta, DR5: cgatttgaggtcaccag-gaggtcacacagt and unr: cggagaagggatccgaactcccaaaca-aac (Langlois et al., 2000) were labeled and incubated for binding as in (Galliot et al., 1995). For supershifts experiments, the polyclonal anti-huCOUP-TF1 T19 antibody (Santa Cruz Biotechnology) was preincubated with 2.5 μl protein lysate for 15 min on ice. Then, 10 fmol of the end-labeled DR5 were added and incubation was continued for 15 min at RT. Samples were loaded on 4% PAGE and run at 150 V at RT with recycling buffer.

Transactivation assays in mammalian cells

Ros 17.2/8 (rat osteosarcoma) cells were maintained in Dulbecco's modified Eagle's medium (DMEM) supplemented with 5% fetal calf serum (FCS). A total of 1.5×10^5 cells in 24-well plates was transfected using 4 μl ExGen500 (Euromedex) with 1.0 μg total DNA including 0.1 μg reporter plasmid, 5 ng of AmphiRAR and AmphiRXR each and increasing amounts of AmphiCOUP (10 to 500 ng) and hyCOUP-chim2 (100 to 1000 ng). AmphiRAR, AmphiRXR, AmphiCOUP and hyCOUP-chim2 were cloned into the pSG5 expression vector (Stratagene). Three tandem repeats of oligonucleotides encompassing consensus DR5 sequence were inserted into the pGL2-promoter vector (Promega). The culture medium was changed 6 h after transfection and all-trans retinoic acid (RA) diluted in DMSO was added (10^{-8} M final). Cells were lysed 24 h after transfection and assayed for luciferase activity.

Results

Isolation of multiple hyCOUP-TF isoforms in hydra

A 117-bp probe corresponding to the hyCOUP-TF C domain was previously obtained from a PCR screen for NR in various metazoans (Escriva et al., 1997) and used for screening a *Hydra vulgaris* (*Hv*) cDNA library. A 981 bp long clone (cDNA type I) was isolated encoding a partial C-domain (60 residues), 81% identical to that of the human COUP-TFI (huCOUP-TF1) protein and a less conserved D domain (Fig. 1A and supplement 1). Upstream to the region encoding the C domain, a 686-bp divergent DNA stretch containing a stop codon at position 663 was found. To obtain full-length cDNAs, the conserved regions of this cDNA were used to screen a second library. Ten distinct new clones were isolated, representing three distinct classes of cDNAs (types II, III, and IV) all encoding ORFs showing similarities with the COUP-TF D and E domains, but

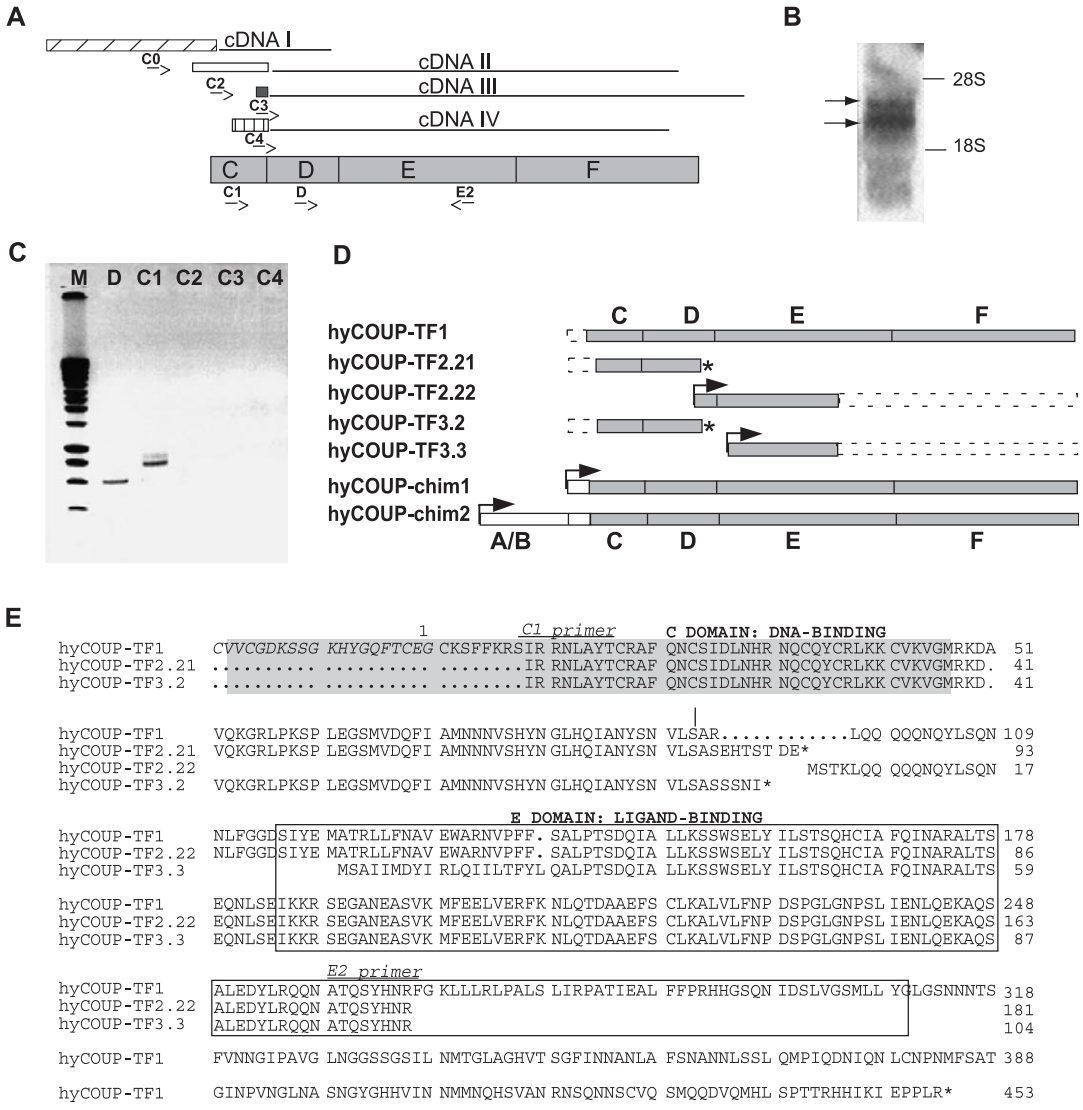

E

```
                                    1          C1 primer      C DOMAIN: DNA-BINDING
hyCOUP-TF1     CVVCGDKSSG KHYGQFTCEG CKSFFKRSIR RNLAYTCRAF QNCSIDLNHR NQCQYCRLKK CVKVGMRKDA  51
hyCOUP-TF2.21  .......... .......... ........IR RNLAYTCRAF QNCSIDLNHR NQCQYCRLKK CVKVGMRKD.  41
hyCOUP-TF3.2   .......... .......... ........IR RNLAYTCRAF QNCSIDLNHR NQCQYCRLKK CVKVGMRKD.  41

hyCOUP-TF1     VQKGRLPKSP LEGSMVDQFI AMNNNVSHYN GLHQIANYSN VLSAR.............LQQ QQQNQYLSQN 109
hyCOUP-TF2.21  VQKGRLPKSP LEGSMVDQFI AMNNNVSHYN GLHQIANYSN VLSASEHTST DE*                    93
hyCOUP-TF2.22                                                      MSTKLQQ QQQNQYLSQN  17
hyCOUP-TF3.2   VQKGRLPKSP LEGSMVDQFI AMNNNVSHYN GLHQIANYSN VLSASSSNI*

                                                E DOMAIN: LIGAND-BINDING
hyCOUP-TF1     NLFGGDSIYE MATRLLFNAV EWARNVPFF. SALPTSDQIA LLKSSWSELY ILSTSQHCIA FQINARALTS 178
hyCOUP-TF2.22  NLFGGDSIYE MATRLLFNAV EWARNVPFF. SALPTSDQIA LLKSSWSELY ILSTSQHCIA FQINARALTS  86
hyCOUP-TF3.3               MSAIIMDYI RLQIILTFYL QALPTSDQIA LLKSSWSELY ILSTSQHCIA FQINARALTS  59

hyCOUP-TF1     EQNLSEIKKR SEGANEASVK MFEELVERFK NLQTDAAEFS CLKALVLFNP DSPGLGNPSL IENLQEKAQS 248
hyCOUP-TF2.22  EQNLSEIKKR SEGANEASVK MFEELVERFK NLQTDAAEFS CLKALVLFNP DSPGLGNPSL IENLQEKAQS 163
hyCOUP-TF3.3   EQNLSEIKKR SEGANEASVK MFEELVERFK NLQTDAAEFS CLKALVLFNP DSPGLGNPSL IENLQEKAQS  87

               E2 primer
hyCOUP-TF1     ALEDYLRQQN ATQSYHNRFG KLLLRLPALS LIRPATIEAL FFPRHHGSQN IDSLVGSMLL YGLGSNNNTS 318
hyCOUP-TF2.22  ALEDYLRQQN ATQSYHNR                                                        181
hyCOUP-TF3.3   ALEDYLRQQN ATQSYHNR                                                        104

hyCOUP-TF1     FVNNGIPAVG LNGGSSGSIL NMTGLAGHVT SGFINNANLA FSNANNLSSL QMPIQDNIQN LCNPNMFSAT 388

hyCOUP-TF1     GINPVNGLNA SNGYGHHVIN NMMNQHSVAN RNSQNNSCVQ SMQQDVQMHL SPTTRHHIKI EPPLR*     453
```

Fig. 1. (A) Scheme depicting the four distinct types of *hyCOUP-TF* cDNAs isolated from *Hydra vulgaris.* These cDNAs encode either the (C) and (D) domains (type I), or the D, E, and F domains (types II, III, and IV) and differ by their unrelated distinct 5′ UTR sequences. The position and the orientation of the C1, C2, C3, C4, D, E2 primers used in the RT-PCR experiment described in C are indicated. (B) Northern analysis of mRNA prepared from intact hydra showing two main bands indicated by arrows. (C) RT-PCR products obtained with each of the forward primers (D, C1, C2, C3, C4) in combination with the E2 primer. Only cDNAs corresponding to D + E (lane D) or C + E (lane C1) domains were amplified. M: marker. (D) Scheme describing the structure of the *hyCOUP-TF* isoforms whose deduced sequences are aligned in E, and the chimeric constructs used in functional assays. The hyCOUP-TF1 isoform, which was confirmed by RT-PCR in C (lane D), was produced by assembling overlapping types I and III cDNAs. Two distinct isoforms were characterized from the RT-PCR products shown in C (C1 lane): hyCOUP-TF2 and hyCOUP-TF3, each of them encoding two distinct putative translation products. For the hyCOUP-chim1 construct, 25 residues including 21 residues of the huCOUP-TFI (C) domain missing in the type I cDNA were inserted in front of hyCOUP-TF1. For the hyCOUP-chim2 construct, the full huCOUP-TF1 N-terminus (A/B and partial C domains) was inserted in front of hyCOUP-TF1. Initiation codons are indicated with horizontal arrows, stop codons with stars. (E) Alignment of the five putative hyCOUP-TF isoforms sequences deduced from the different cDNAs (given in supplement 1) and the three distinct RT-PCR product sequences (given in supplement 3). Residues in italics correspond to the human N-terminal part of the C-domain (grey background). Accession numbers: *hyCOUP-TF1*: Y690637; *hyCOUP-TF2*: Y690638; *hyCOUP-TF3*: Y690639.

lacking the C domain (Fig. 1A and supplements 1 and 2). Thus, these cDNAs only shared the D domain with the cDNA type I. These three types of cDNAs exhibited variable and divergent 5′ sequences, bearing no sequence identity to any sequence, but containing stop codons and thus likely representing non-coding sequences (described in supplement data). Surprisingly, these 5′ sequences diverged at the exact same position, at the boundary between the C and D domains (position 831 in cDNA type I, supplement 2B).

To confirm the presence of such transcripts, RT-PCRs on total RNA from hydra lower halves taken 3h after bisection were performed using specific primers located along the C (C1), D (D), and E (E2) domains and on the four divergent 5′ sequences of cDNAs type I, II, III, and IV (C0, C2, C3, C4, respectively, Fig. 1A). The RT-PCRs that used primers

located at the 5′divergent regions failed to amplify any DNA fragment (Fig. 1C and not shown). Moreover, despite several attempts (inverted PCR, genomic library screening, PCR with conserved oligonucleotides), we were unable to isolate the corresponding genomic region. Since the divergent 5′regions of the various cDNAs were not detected by RT-PCR, we suspect that these cDNAs represented chimeric cDNA library artifacts. In contrast, the RT-PCRs that used the D + E2 primers detected one main PCR product while at least two distinct products were detected with the C1 + E2 pair of primers (Fig. 1C). Interestingly, Northern analysis detected two main bands in the range of 3 and 3.5 kb, confirming thus the presence of at least two distinct *hyCOUP-TF* transcripts in hydra (Fig. 1B). The molecular characterization of the C1 + E2 RT-PCR products detected three distinct isoforms: *hyCOUP-TF1*, which encodes the C, D and E domains previously characterized in cDNAs type I–IV; *hyCOUP-TF2*, which contains a 131-bp deletion within the D region and finally, *hyCOUP-TF3*, which shows a 156-bp insertion also within the D region (Figs. 1D, E, and supplement 3). Translation of hyCOUP-TF2 and hyCOUP-TF3 isoforms generates stop codons that produce truncated hyCOUP-TF proteins lacking the E domain, hyCOUP-TF2.21, and hyCOUP-TF3.2, respectively. Alternatively, these isoforms could also generate truncated hyCOUP-TF proteins that would contain only the E domain, hyCOUP-TF2.22 displaying an initiation codon in the D domain and hyCOUP-TF3.3 showing an initiation codon and a divergent sequence up to position 25 of the E domain. Therefore, given that RT-PCR experiments could detect transcripts where the regions encoding the C and E domains were linked, but in the absence of characterized *hyCOUP-TF* 5′ end, we decided to fuse the C–F domains obtained in types I and III cDNAs in a construct named hyCOUP-TF1. HyCOUP-TF1 was further used to construct chimeric human-hydra COUP-TF clones (Fig. 1D), which would contain either a complete C domain (hyCOUP-chim1) or a complete N-terminus with the addition of the human A/B domain (hyCOUP-chim2).

Conservation of the COUP-TF functional domains from cnidarians to vertebrates

The Blast search provided hyCOUP-TF-related sequences that all belong to the class II NR: COUP, RXR, HNF4, TLL, TR2/4 (Nuclear Receptor Nomenclature Committee, 1999). When the COUP-TF C, D and E domains were aligned (Fig. 2), the overall identity of hyCOUP-TF was 47% with huCOUP-TFI, 45.7% with the human COUP-TFII, 43.8% with the coral AmNR7, 42.9% with the human EAR2 orphan receptor, and 44.6% with the *Drosophila* SVP protein. These values reached 55% when conservative substitutions were taken into account. By comparison, the identity level was only 30.7% with the jellyfish RXR indicating that we isolated a hydra gene representative of the COUP-TF gene family. Phylogenetic analyses performed either on the C–E domains (318 residues, Fig. 3) or on the C domain (60 residues, not shown) of 51 class II NR protein sequences confirmed that hyCOUP-TF is indeed a member of the COUP-TF group. However, the coral COUP-TF homolog (AmNR7, Grasso et al., 2001) exhibited a far more conserved sequence than the hyCOUP-TF, 80% identical to the huCOUP-TF in the C–E domains. In hyCOUP-TF, the C domain is the most conserved one, reaching 81 to 83% identity with vertebrate COUP-TF C domains. Among the different isolated cDNAs, the hyCOUP-TF type I was the only one to contained a C domain, although partial because lacking the 21 N-terminal amino acids when compared to the huCOUP-TF1, including the three first cysteines of the first zinc finger (Fig. 2). The similarity to NR actually started inside the recognition helix (CEGCKSFFKRSVR) a highly conserved motif, which mediates the direct interaction of the receptor to the major groove of the DNA double helix (Holmbeck et al., 1998; Zhao et al., 2000). Similarly, the second helix displays a very high level of conservation (positions 34–45 in Fig. 2). A very strong pressure was thus maintained along evolution on residues that are critical to the DNA-binding function. These observations strongly argue in favor of the fact that a regular COUP-TF protein, that is, containing a complete and functional DNA-binding domain, is present in hydra.

The E domains from hyCOUP-TF and huCOUP-TFI harbor 44% sequence identity (Fig. 2). The homology is scattered over nine regions that roughly correspond to the α-helices determined by the 3D structure resolution of the RARα and RXR E domains (Bourguet et al., 1995; Renaud et al., 1995). This suggests that hyCOUP-TF, as its homologs in other metazoans, will fold in a common tertiary structure (Wurtz et al., 1996). The last remarkable feature of hyCOUP-TF is the presence of a long F domain, C-terminal to the E domain. This domain does not show identity to any other proteins. F domains are not uncommon in NRs although their functions often remain elusive (reviewed in Laudet and Gronemeyer, 2002).

hyCOUP-TF and prdl-b are both expressed in the nematocyte and the neuronal cell lineages

In situ hybridizations were performed with a *hyCOUP-TF* riboprobe corresponding to the D and E domains and thus less prone to cross-hybridize with other nuclear receptor genes expressed in hydra. In adult polyps, *hyCOUP-TF* was expressed as ectodermal multicellular spots in the body column, but absent from the apical and basal regions (Figs. 4A–C). Rare scattered groups of *hyCOUP-TF* expressing cells were detected in the peduncle and upper body column. This body column pattern was observed in budless polyps as well as in late-stage buds. *HyCOUP-TF* expressing cells were clustered in nests of 2 to 16 cells, identified as dividing and differentiating nematoblasts (Figs. 4C and 5A–F). In heavily stained animals, we detected a second population of *hyCOUP-TF* expressing

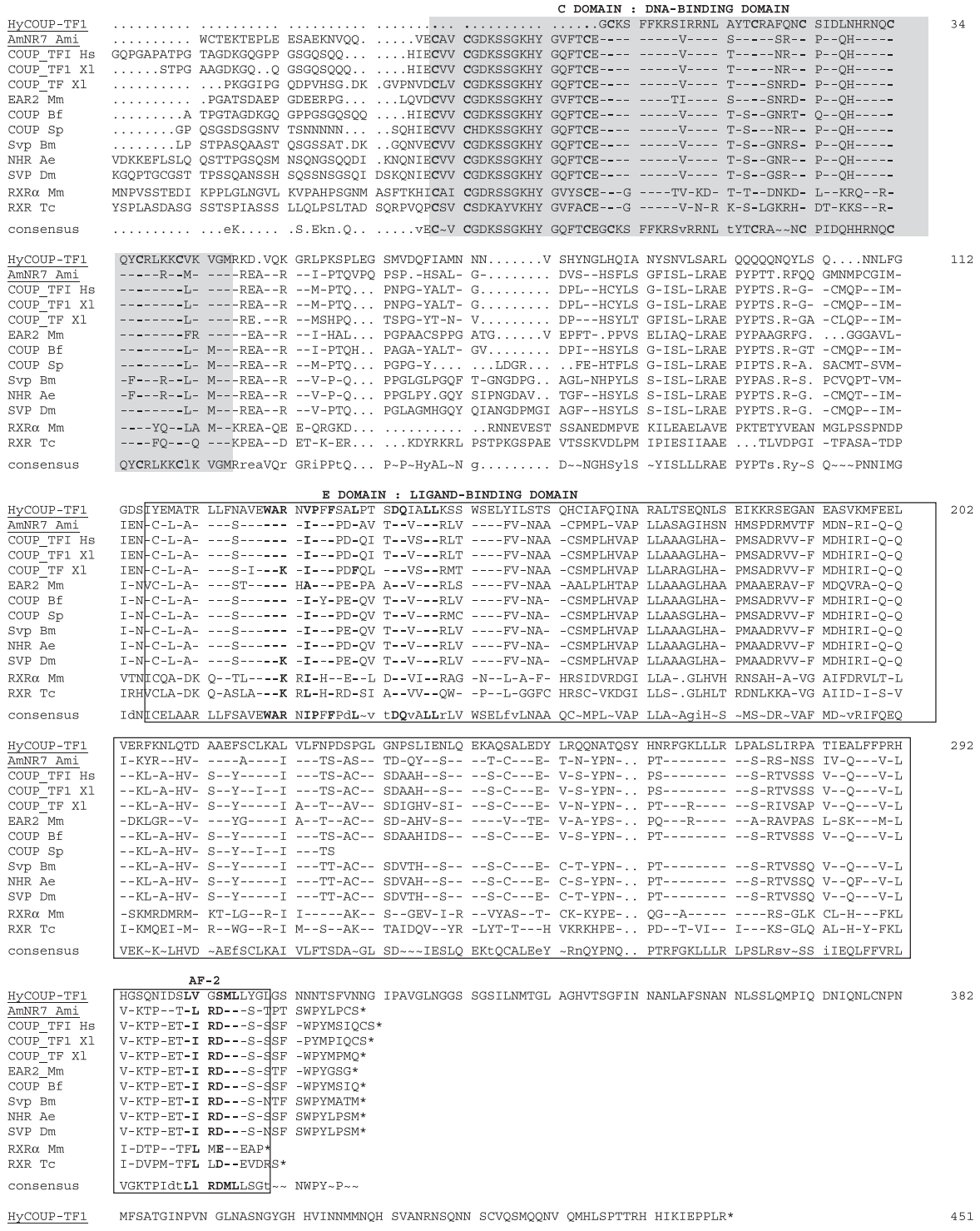

Fig. 2. Alignment of various COUP-TF group members with the cnidarian COUP-TF homologs, hyCOUP-TF1, and AmNR7. Identical amino acid positions are indicated by dashes, dots correspond to gaps. The A/B and F regions were not included since too variable. The C domain is shaded in grey and the E domain is boxed. A consensus that shows residues conserved from cnidarians to bilaterians was derived, residues written in lowercase indicating conservative substitutions. Accession numbers of the various sequences: *HyCOUP-TF*: U93425; *AmNR7*: tr|Q95WF7; *COUP_TF1 Hs*: sp|P10589; *COUP_TF1 Xl*: tr|Q9W745; *COUP_TF Xl* tr|Q91720; *EAR2 Mm*: sp|P43136; *COUP Bf*: AY211769; *COUP Sp*: tr|Q26641; *Svp Bm*: tr|Q969A9; *NHR-Ae* tr|Q9BMU6; *SVP Dm*: sp|P16375; *RXRα Mm*: X66223; *RXR Tc*: AF091121. For species code see Fig. 3.

cells located deeper than the nests of nematoblasts, along the mesoglea (Fig. 4D), appearing as small and single cells most often exhibiting long processes characteristic of neuronal cells (Fig. 4E). These neuronal *hyCOUP-TF* expressing cells were also observed in the hypostome region (Fig. 4D). Similarly to *hyCOUP-TF*, the *prdl-b* transcripts were

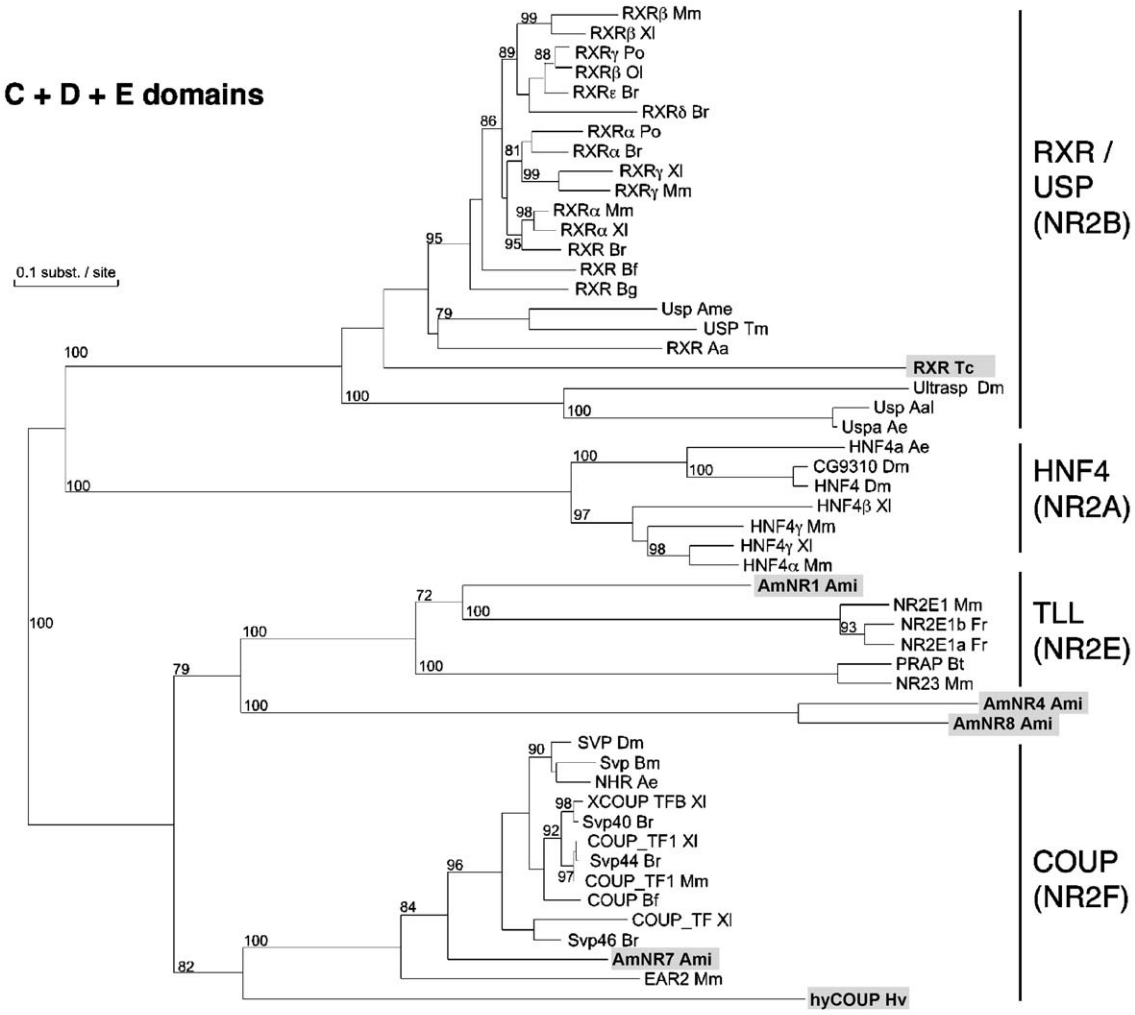

Fig. 3. Phylogenetic relationships among 51 nuclear receptor sequences representing the COUP, RXR, HNF4, TLL families obtained by Neighbor-Joining method (Saitou and Nei, 1987) with a PAM-Dayhoff matrix (Dayhoff et al., 1978). Cnidarian sequences are written bold case and boxed in grey. The tree was constructed with the C–E domains (318 residues after pairwise gap removal). Bootstrap values above 80% (500 replicates) are indicated. Species code: *Aa: Amblyomma americanum*; *Aal: Aedes albopictus* (forest day mosquito); *Ae: Aedes aegypti* (yellowfever mosquito); *Ame: Apis mellifera* (honeybee); *Ami: Acropora millipora* (coral); *Bf: Branchiostoma floridae* (amphioxus); *Bg: Biomphalaria glabrata* (bloodfluke planorb); *Bm: Bombyx mori* (silk moth); *Br: Brachydanio rerio* (zebrafish); *Bt: Bos taurus* (bovine); *Fr: Fugu rubripes* (pufferfish); *Dm: Drosophila melanogaster* (fly); *Hs: Homo sapiens* (human); *Hv: Hydra vulgaris; Mm: Mus musculus* (mouse); *Ol: Oryzia latipes* (medaka fish); *Pm: Petromyzon marinus* (sea lamprey); *Po: Paralichthys olivaceus* (flounder); *Sp: Strongylocentrotus purpuratus* (sea urchin); *Tc: Tripedalia cystophora* (jellyfish); *Tm: Tenebrio molitor* (yellow mealworm); *Xl: Xenopus laevis* (African clawed frog). The sequence alignment used for the construction of this tree is available in supplement 4.

detected in nests of cells spread along the body column, but absent from the apical and basal regions of the adult polyps (Figs. 4F, G) as previously described (Gauchat et al., 1998; Miljkovic-Licina et al., in press). Interestingly, we also observed *prdl-b* expression in pairs of small dividing interstitial cells (Fig. 4H), and in small single cells, some of them displaying processes typical of neuronal cells (Fig. 4I). This *prdl-b* expression in the nerve cell lineage, which is more easily detected with fluorescent staining, was initially overlooked because of the massive expression in the nematoblasts. Therefore, in hydra *hyCOUP-TF* and *prdl-b* are expressed in two distinct lineages that differentiate from a common interstitial stem cell (Bode, 1996). In fact, it was proven that apical and basal regions exhibit an inhibitory influence on nematocyte differentiation, which as a consequence, is excluded from these regions and restricted to the ectodermal layer of the body column (Bode, 1996; Fujisawa et al., 1986). In contrast, there is no restriction for neuronal differentiation.

HyCOUP-TF and prdl-b show partially overlapping cellular distributions in the nematocyte lineage

To test whether *prdl-b* and *hyCOUP-TF* were co-expressed at similar stages in the nematocyte lineage, we carried out double in situ hybridizations with the *prdl-b* and *hyCOUP-TF* riboprobes (Figs. 4J–L). Colocalization of the *hyCOUP-TF* (green) and the *prdl-b* (red) signals was clearly

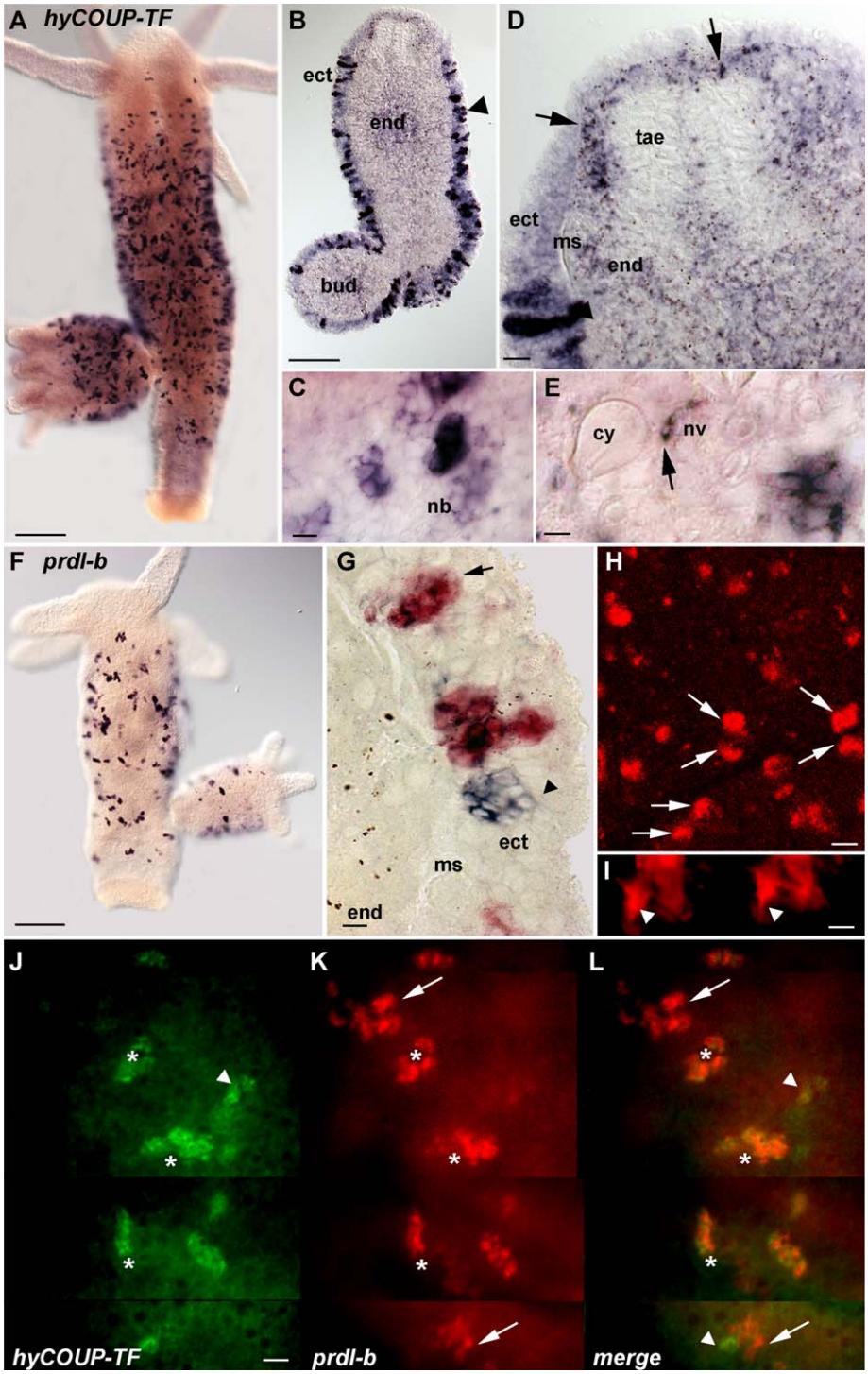

Fig. 4. *HyCOUP-TF* (A–E) and *prdl-b* (F–I) are expressed in both the nematocyte and neuronal cell lineages. (A) *hyCOUP-TF* expression pattern in hydra polyp. (B, D) DIC views of cryosections performed after whole mount ISH. (B) Expression of *hyCOUP-TF* in nests of nematoblasts (arrowhead) restricted to the body column of adult and budding polyps. (C) Enlarged view of the body column showing nests of *hyCOUP-TF* expressing cells. (D) Enlarged view of the apical region of the animal depicted in B showing scattered single small *hyCOUP-TF* expressing cells in the head region (arrows). (E) Neuronal cell (nv) expressing *hyCOUP-TF* (arrow). (F) *prdl-b* expression pattern in hydra polyp. (G) DIC view of a cryosection performed after double whole mount ISH where *prdl-b* expressing cells are red (arrow) and *hyCOUP-TF* blue (arrowhead). (H) Confocal view of single cells and mitotic pairs of interstitial cells expressing *prdl-b* (arrows). (I) Confocal views of a single cell displaying processes typical of neuronal cells (arrowhead). (J–L) Co-localization of nests expressing *hyCOUP-TF* (green) and/or *prdl-b* (red). Arrowheads indicate nests expressing *hyCOUP-TF* but not *prdl-b*, arrows point to nests expressing *prdl-b* but not *hyCOUP-TF* and stars label nests that co-express *hyCOUP-TF* and *prdl-b*. cy: nematocyst, ect, ectoderm; end, endoderm; ms, mesoglea; nb, nematoblasts; tae: taeniolae. Scale bars: 400 μm in A, B, F; 50 μm in D; 20 μm in C, G; 7 μm in E; 64 μm in J–L; 3.6 μm in H; 1.8 μm in I.

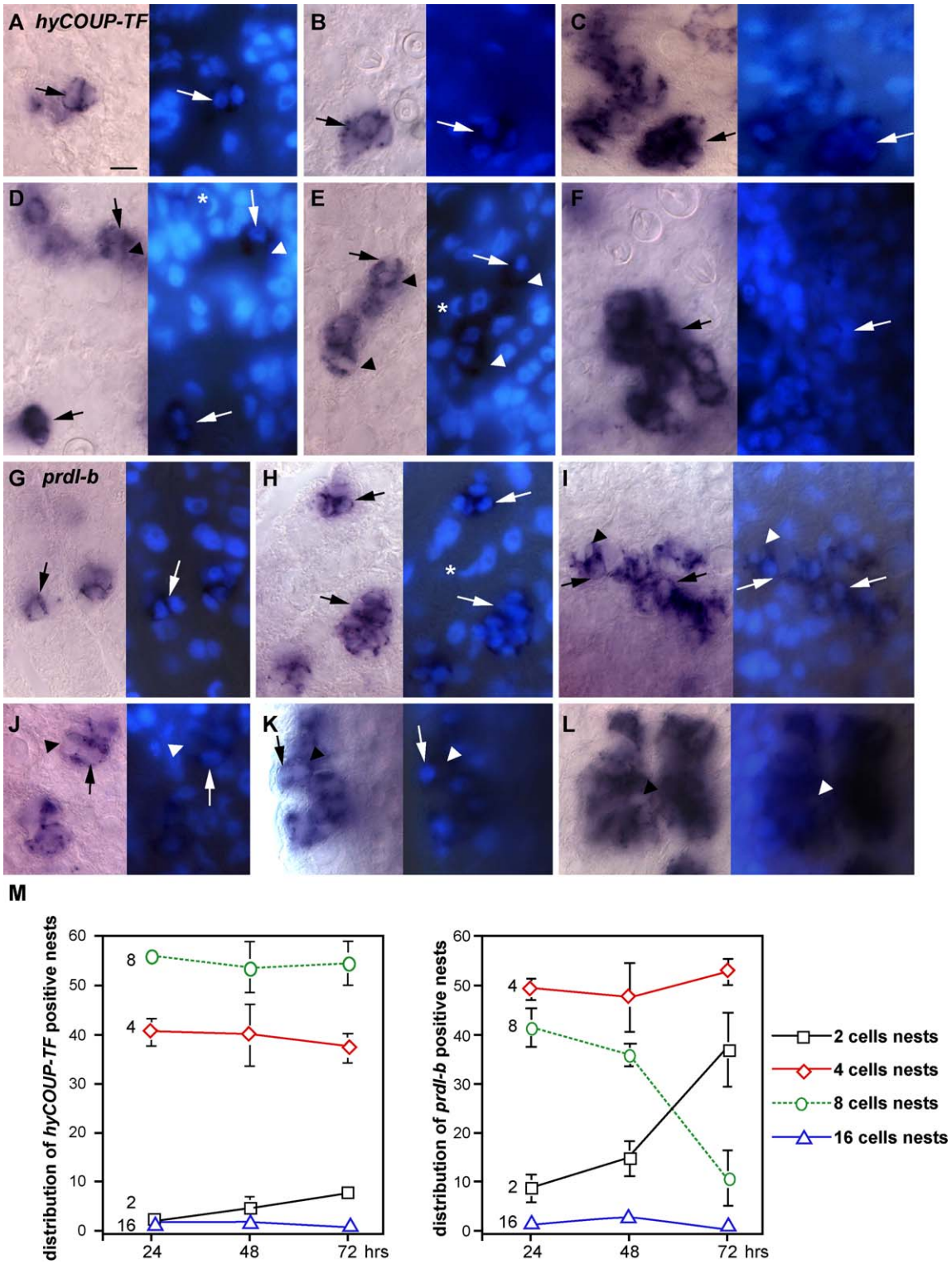

Fig. 5. Analysis of *Hm 105* dividing nematoblasts and differentiating nematocytes expressing *hyCOUP-TF* (A–F) and *prdl-b* (G–L). Expression of both genes was detected in 2 (A, D, G), 4 (B, E, H), 8 (C), and 16 (C, F, I, L) cell clusters. Arrows point to nuclei, arrowheads to nematocysts in D, E, I–L, stars indicate "moon-shape" nuclei of mature nematocytes. DAPI staining in right panels. Scale bar: 20 μm. (M) Distribution of *hyCOUP-TF* (left panel) and *prdl-b* (right panel) expressing nests according to their size after 24, 48, and 72 h of starvation.

observed in a large subset of cells (stars), reaching 85 ± 11.3% of the nests in case of *prdl-b* but only 63 ± 7.6% in case of *hyCOUP-TF*. This difference reflects the fact that *hyCOUP-TF* is expressed in a larger number of nests than *prdl-b*. In fact, 37% of the *hyCOUP-TF* nests did not express *prdl-b* (Figs. 4J–L, arrowheads), while 15% of the

prdl-b nests did not express *hyCOUP-TF* (Figs. 4J–L, arrows). We furthermore identified more precisely the stages of the nematocyte pathway where *hyCOUP-TF* and *prdl-b* were expressed, by counting the distribution of the *hyCOUP-TF* and *prdl-b* expressing nests according to their size in animals fixed 24 h after the last feeding (Fig. 5). *HyCOUP-TF* and *prdl-b* were detected in nests of 2 to 16 cells (Figs. 5A–L), 4 and 8 cell clusters representing over 80% of the positive nests for both genes (Fig. 5M). Moreover, a comparative analysis of DIC views and DAPI staining showed that, beside the nucleus, a typical differentiating capsule could be observed in about 30% of the *hyCOUP-TF* and *prdl-b* expressing nests (Figs. 5D–F, I–L, arrowheads), proving that *hyCOUP-TF* and *prdl-b* transcripts are still present at the differentiation stage. However, *hyCOUP-TF* and *prdl-b* transcripts were never detected in nematocytes displaying a fully mature nematocyst, which displays a typical moon-shaped nucleus (Figs. 5D, E, H, stars). Besides these similarities, we noted some clear-cut differences between the *hyCOUP-TF* and *prdl-b* cell populations: first, the most abundant nests were the 8 cell clusters in case of *hyCOUP-TF*, representing about 55% of all nests, instead of the 4 cell clusters in case of *prdl-b* that represent about 50% of all nests (Fig. 5M). Second, 2 cell clusters were more frequently detected among *prdl-b* expressing nests, representing 8.5% of total nests versus 1.7% in case of *hyCOUP-TF* (Fig. 5M). These results prove that *hyCOUP-TF* and *prdl-b* are largely co-expressed in dividing nematoblasts; nevertheless *hyCOUP-TF* expression is likely initiated in nematoblasts having undergone at least two rounds of cell divisions (4 cell clusters) while *prdl-b* expression is initiated at two different stages, first earlier than *hyCOUP-TF* in pairs of interstitial cells and at a later stage in 4 cell clusters. This result is in agreement with our previous findings, according to which, *prdl-b* expression was detected in the small interstitial cell fraction by elutriation (Gauchat et al., 1998). These pairs of interstitial cells represent dividing stem cells as well as precursors to nematoblasts and neuronal cells (Bode, 1996; Holstein and David, 1990). The 2 cell clusters that express *hyCOUP-TF* and/or *prdl-b* could thus represent three distinct subpopulations, interstitial stem cells, precursors to nematoblasts, and precursors to neuronal cells.

HyCOUP-TF and prdl-b expressing cells show distinct regulations upon starvation

In the epithelial cell lineage, starvation does not lead to arrest of cell proliferation (Bosch and David, 1984) but rather induces on one hand an increase of the cell cycle length resulting in a 2-fold decrease of BrdU-labeled cells in the body column (Holstein et al., 1991) and on the other hand, a phagocytotic process (Bosch and David, 1984), following a typical apoptotic process (Cikala et al., 1999). Hence, starvation results in dramatic cellular rearrangements. To compare the specific regulations of *hyCOUP-TF* and *prdl-b* expressing nests in this context, we measured their respective distributions according to the size of the nests after 1, 2, or 3 days of starvation (Fig. 5M). The distribution of *hyCOUP-TF* expressing nests showed a dramatic 4.5-fold increase from 1.7 ± 0.5% to 7.6 ± 1.5% in the number of 2 cell clusters after 3 days of starvation. Similarly, in case of the *prdl-b* gene, we recorded a 4.3-fold increase in the number of 2 cell clusters from 8.5% ± 2.9 to 36.8% ± 7.5. However, in case of *hyCOUP-TF*, we did not register any significant variation in the number of 4 and 8 cell clusters. In contrast, in case of *prdl-b* together with the increase in 2 cell clusters, we noted a symmetrical 4.1-fold decrease in the number of 8 cell clusters from 41.4 ± 3.9% to 10.5 ± 5.6% and a complete disappearance of the 16 cell clusters but no variation of the 4 cell clusters. As previously mentioned, the two cell clusters are composed of two distinct cell populations: the interstitial stem cells, characterized by a short cell cycle and the early precursors to several differentiation pathways, among which the precursors to nematocyte differentiation, which are medium-cycle cells (Holstein and David, 1990). At subsequent stages, the nematoblast nests are characterized by a tightly tuned coordination between a variable number of synchronous divisions followed by the differentiation of the capsule, which is also a synchronous process within a nest (Bode, 1996). Consequently, the growth rate of the nematoblast population is the result of an equilibrium between the number of synchronous divisions, the stage where nematoblasts enter the differentiation process, and possibly the magnitude of the apoptotic process (Fujisawa and David, 1984). According to these parameters, we can propose the following explanations for the observed results: First, the dramatic increase in the ratio of 2 cell clusters expressing *hyCOUP-TF* and *prdl-b* can be explained by the fact that the division rate of stem cells, which are short-cycling cells (Holstein and David, 1990), is not affected upon starvation, while precursors to nematocyte differentiation, which are medium-cycling cells (Holstein and David, 1990), display a cell cycle lengthened upon starvation. The combination of these two mechanisms would lead to an increase in the pairs of interstitial cells. Second, the absence of variation in the fraction of 4 cell clusters expressing *hyCOUP-TF* can simply be explained by the lengthening of the cell cycle of nematoblasts whatever their stage: the number of 4 cell clusters produced from 2 cell clusters is lower but assuming that the cell cycle length is also increased upon starvation in 4 cell clusters (the traverse of the 4 cell stage takes longer), then the number of 4 cell clusters expressing *hyCOUP-TF* will stay stable providing that initiation of *hyCOUP-TF* expression is maintained in 4 cell clusters, which seems to be the case. Similar reasoning applies to the 8 cell clusters expressing *hyCOUP-TF*. Third, the absence of variation in the fraction of 4 cell clusters expressing *prdl-b* could be explained the same way. However, the clear-cut decrease in 8 cell clusters and the disappearance of 16 cell clusters expressing *prdl-b*, should be differently addressed. Either

hyCOUP-TF and *prdl-b* are submitted to distinct regulations within a homogenous cell population, or their specific regulations reflect the regulation of two distinct sub-populations. As we found a partially overlapping cellular expression, both possibilities should be discussed. In the case of a homogenous cell population, the formation of 4 and 8 cell clusters is slowed down but not quantitatively altered upon starvation suggesting that either *prdl-b* expression is drastically and specifically down-regulated in the 8 cell clusters and absent in 16 cell clusters. In the case of distinct subpopulations, either as a consequence of the lengthening of the cell cycle the *prdl-b* expressing 4 cell clusters will differentiate earlier before reaching mitosis, thus preventing the formation of 8 and 16 cells, or 8 and 16 cell clusters upon starvation will dissociate providing transiently smaller nests (4 cells, 2 cells, and single cells).

BrdU labeling index of hyCOUP-TF and prdl-b-expressing cells are different

To better characterize the *hyCOUP-TF* and *prdl-b* expressing cell populations, we investigated their respective rates of proliferation by incubating hydra (*Hm 105*) with BrdU for either 1, or 24 or 48 h to visualize cells that went through S phase. Animals were subsequently fixed and processed for in situ hybridization followed by anti-BrdU immunohistochemistry (Figs. 6A, B) and the percentage of labeled cells (BrdU labeling index) among the *hyCOUP-TF* and *prdl-b* expressing nests was counted (Fig. 6C). After 1 h labeling, the BrdU labeling index was null for the 2 cell populations, probably because the animals were 24 h starved. In the case of *hyCOUP-TF*, the BrdU labeling index reached 50% after 24 h whatever the size of the nests and was over 80% in the 4 and 8 cell clusters after 48 h. Interestingly, the BrdU labeling index of 2 cell clusters did not increase after 24 and 48 h, suggesting that at least 50% of the *hyCOUP-TF* 2 cell clusters are either slower cycling cells or are not cycling at all, which corresponds with our assumption that these cells might represent precursors to neuronal cells. In case of *prdl-b*, only 35% of the 2 cell clusters were labeled after 24 h whereas 95% of the 4 and 8 cell clusters were already BrdU labeled at that time. This result is in agreement with the heterogenous cell populations found among 2 cell clusters: on one side the stem cells that are fast-cycling and on the other the precursors of the neuronal and nematocyte lineage, which are cycling at a lower rate, specially when animals are starving. In comparison 4 and 8 cell clusters expressing either *hyCOUP-TF* or *prdl-b* represent synchronous cell populations with almost identical BrdU labeling index at 24 and 48 h. However, these two cell populations display significantly different BrdU labeling index at 24 and 48 h, respectively. At 48 h, while all *prdl-b* expressing nests went through S phase, this does not seem to be the case for all *hyCOUP-TF* expressing nests, as 15% to 20% of the 4 and 8 cell clusters did not. This percentage might represent the nests that escaped from proliferation and entered the differentiation process. Thus, these data indicate that these two cell

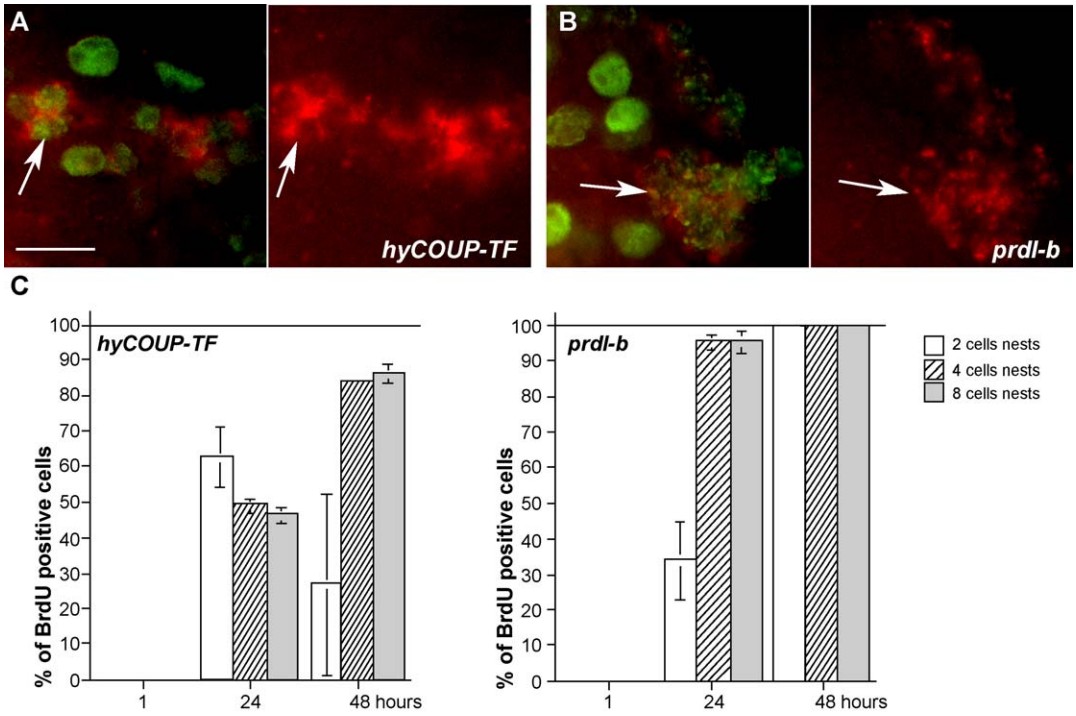

Fig. 6. (A, B) BrdU labeling of *hyCOUP-TF* (A) and *prdl-b* (B) expressing cells after 16 h exposure. Scale bar: 20 μm. (C) *hyCOUP-TF* and *prdl-b* expressing cell clusters show distinct BrdU labeling index after 24 and 48 h exposure.

populations are not identical, as a significant subset of *hyCOUP-TF* expressing nests are no longer cycling, which is not the case of *prdl-b* expressing nests.

In the sf-1 mutant, elimination of the interstitial cell lineage correlates with the disappearance of the hyCOUP-TF and prdl-b-expressing cells

To test whether expression of the *hyCOUP-TF* and *prdl-b* genes was indeed linked with the differentiation of the interstitial cell lineage, we used the temperature sensitive sf-1 mutant that eliminates interstitial cells when animals are maintained above 23°C (Marcum et al., 1980; Terada et al., 1988). After 2 days at 26°C, ISH was performed and expressing nests were counted (Fig. 7). A normal *hyCOUP-TF* and *prdl-b* expression pattern (Figs. 7A, C) was never observed in animals maintained at 26°C. Instead, two distinct phenotypes were observed when compared to animals maintained at 18°C, a weak one where few expressing nests were recorded and a null one where we

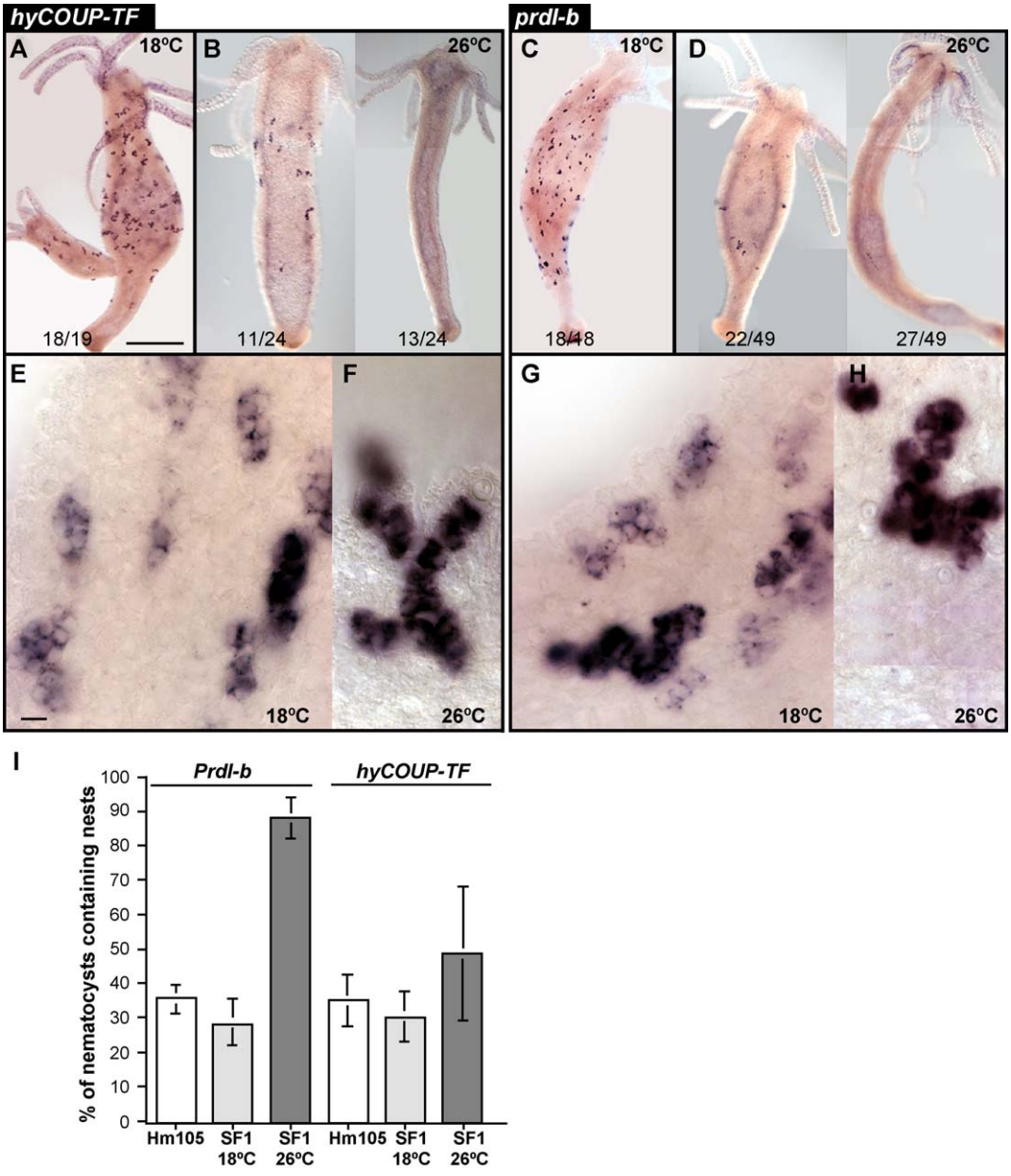

Fig. 7. *HyCOUP-TF* and *prdl-b* expressing cells are eliminated in the sf-1 mutant hydra maintained at 26°C. (A, C) Sf-1 mutant animals maintained at permissive temperature (18°C) and tested for *hyCOUP-TF* (A) and *prdl-b* (C) expression. (B, D) Sf-1 mutant animals maintained at non-permissive temperature (26°C) and tested for *hyCOUP-TF* (B) and *prdl-b* (D) expression. (E–H) *HyCOUP-TF* and *prdl-b* expressing nests observed in sf-1 mutant animals maintained either at permissive (E, G) or at non-permissive (F, H) temperatures for 2 days. Scale bars: 1 mm in A–D; 20 μm in E–H. (I) Elimination of interstitial cells leads to a dramatic increase of nematocysts-containing nests in residual *prdl-b* and *hyCOUP-TF* expressing cells.

were unable to detect any expressing cells (Figs. 7B, D). At permissive temperature (Figs. 7E, G), nests of various sizes expressed *hyCOUP-TF* and *prdl-b*, while at non-permissive temperature where interstitial cells are eliminated, only few large size nests that strongly expressed *hyCOUP-TF* and *prdl-b* could be detected in animals displaying a weak phenotype (Figs. 7F, H). The number of animals displaying one or the other phenotype was very similar for the *hyCOUP-TF* and *prdl-b* genes: around 45% for the weak phenotype and 55% for the null phenotype. When we screened for the presence of nematocysts in the expressing nests still present in the animals displaying the weak phenotype, we observed a dramatic increase in the percentage of nematocysts containing nests, over 85% in the case of *prdl-b*, around 50% in the case of *hyCOUP-TF* compared to the 30% usually observed in wild type animals (Fig. 7I). It was actually shown that, while 2 cell clusters are quickly eliminated within the first 12 h after the temperature switch, the number of nematoblasts and nematocytes will not be affected within the first 2 days (Terada et al., 1988). Thus, our results are in agreement with this finding as we observed predominantly large nests of differentiating nematoblasts after 2 days. The difference observed between the *prdl-b* and *hyCOUP-TF* expressing cells indicate that *prdl-b* transcripts persist longer than *hyCOUP-TF* transcripts in cell clusters that entered differentiation. This might occur independently of the elimination process.

HyCOUP-TF and prdl-b are no longer expressed in the nematocyte lineage during morphogenetic processes

We recorded a similar regulation of the *hyCOUP-TF* and *prdl-b* genes in regions undergoing budding, regeneration and sexual development, that is, a clear exclusion of the *hyCOUP-TF* and *prdl-b* transcripts from these regions (Figs. 8 and 9), analogous to the regulation we observed in apical and basal regions of the adult polyp. At early stages of budding (staging according to (Otto and Campbell, 1977), *hyCOUP-TF* and *prdl-b* were first repressed in a limited area of the parental body column, the bud spot, from which the bud will emerge (Figs. 8A, B, H), then in the most distal part of the bud, which corresponded to the presumptive head region (Figs. 8C–G, I–K). From stage 4, we recorded a *hyCOUP-TF* expression in the body column of the emerging bud at the same level as in the parental body column. From stage 8, we observed an exclusion of *hyCOUP-TF* in the proximal region of the bud, which starts differentiating the basal disc (Figs. 8G, K, arrowheads). During regeneration, *hyCOUP-TF* and *prdl-b*-expressing cells immediately vanished from the healing region after amputation (Fig. 8L and not shown), and did not reappear at subsequent stages in apical and basal regenerating stumps (Figs. 8M–Q). This observation is in agreement with the fact that cells of the nematocyte pathway rapidly disappear from regenerating tips without completing differentiation under the inhibitory influence of the de novo developing structure (Yaross and Bode, 1978). Cell death was actually recorded in the regenerating area during head and foot regeneration, a process which affects differentiating but not proliferating nematoblasts (Fujisawa and David, 1984). In the remaining part of the body column, expression of *hyCOUP-TF* and *prdl-b* was not altered and the boundary between the expressing domain in the body column and the "empty" area in the regenerating stump was rather sharp (Fig. 8, arrows). In addition, in the regenerating stump area, proliferation of epithelial cells is inhibited, forming an "empty" growth-arrested area during the first day of regeneration (Holstein et al., 1991). Thus, this mitotic inhibition likely also affects proliferation of nematoblasts. During gametogenesis and early developmental stages, we could not detect any *hyCOUP-TF* or *prdl-b* expression (Fig. 9): *hyCOUP-TF* and *prdl-b* transcripts were detected neither in testes (Figs. 9A, B, G, H), nor in oocytes (Figs. 9D, E, I, J), nor in developing embryos (Figs. 9C, F). In female polyps, *hyCOUP-TF* was also found transiently repressed in the region of the parental body column facing either the oocyte or the developing embryo. Thus, here *hyCOUP-TF* and *prdl-b* display highly similar regulations of their expression in the nematocyte pathway, that is, a complete exclusion from regions where developmental programs are activated.

HyCOUP-TF behaves as a repressor in mammalian cells

COUP-TF transcription factors bind to evolutionarily conserved DNA motifs and behave in most contexts as potent negative transcriptional regulators (Giguere, 1999; Tsai and Tsai, 1997). To define the putative function of hyCOUP-TF, we first tested the specific DNA-binding activity of the hyCOUP-chimeric constructs, hyCOUP-chim1 and hyCOUP-chim2 (Fig. 10A). We were unable to detect any specific DNA-binding activity of hyCOUP-chim1, while competition experiments proved that hyCOUP-chim2 provided a specific DNA-binding activity onto both the DR1 and DR5 consensus elements. This result proves that the hydra C domain efficiently and specifically binds to DNA when the A/B domains are present, suggesting that the A/B domains contribute to the stabilization of the DNA/C domain interactions. In the presence of the T19 antibody raised against the N-terminus of the huCOUP-TF1 protein, a supershift was clearly observed (Fig. 10A, lanes 11, 12, 17, 18) with hyCOUP-chim2. COUP-TF from amphioxus (amphiCOUP-TF) was used as a positive control in this experiment (Langlois et al., 2000). As expected, the complex formed by amphiCOUP-TF onto DR5 was not supershifted in the presence of the T19 antibody (Fig. 10A, lanes 19–23).

In COUP-TFs, transcriptional repressor activity was mapped within the E domain (Achatz et al., 1997). As this E domain is conserved in hyCOUP-TF, we tested whether hyCOUP-TF could repress the RAR:RXR transcriptional

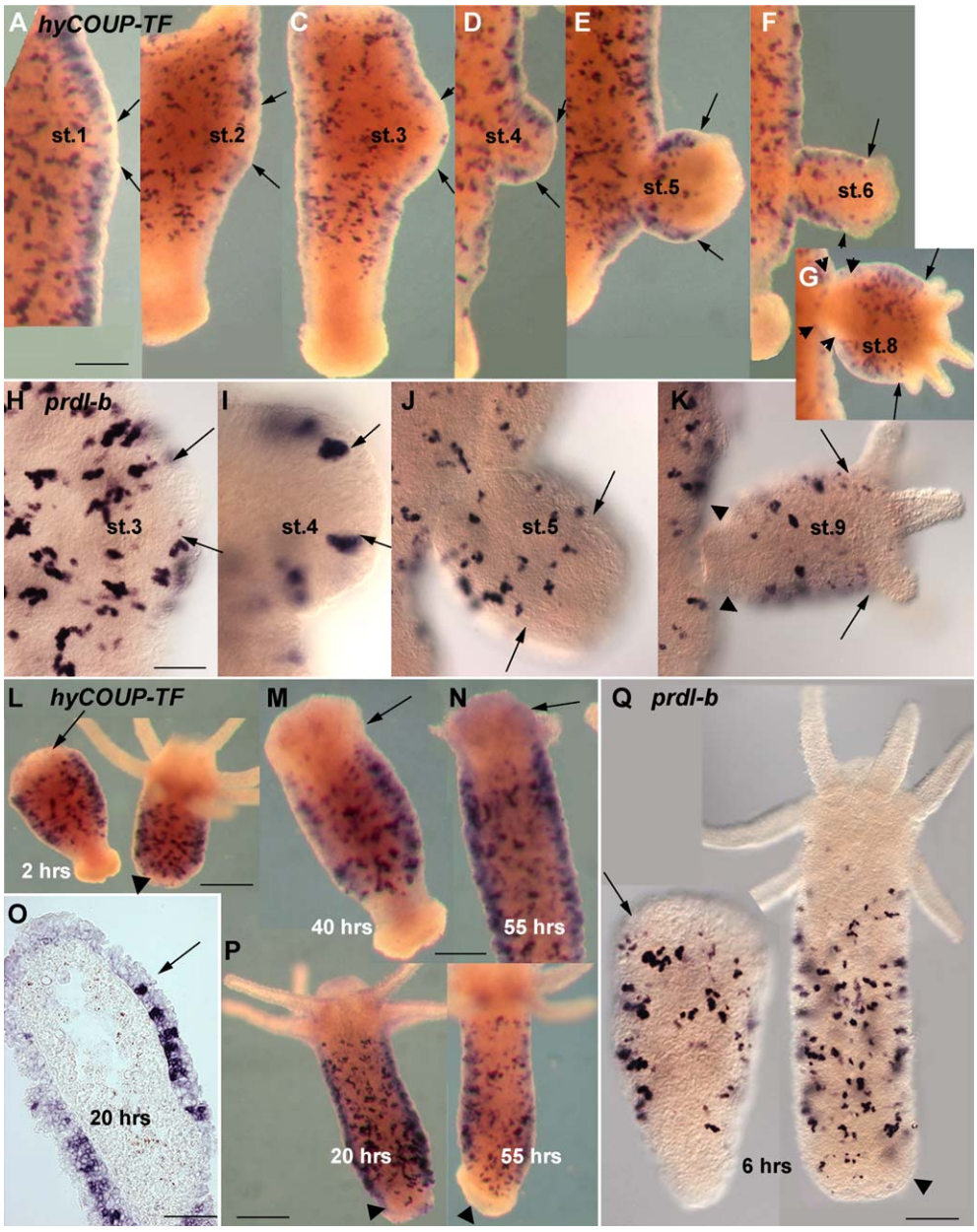

Fig. 8. Exclusion of *hyCOUP-TF* and *prdl-b* expressing cell clusters in budding (A–K) and regenerating (L–Q) areas. *HyCOUP-TF* (A–G) and *prdl-b* (H–K) expressing nests in budding hydra from stage 1 to stage 9 according to Otto and Campbell (1977). Arrows indicate the boundaries of the excluded regions. *HyCOUP-TF* (L–P) and *prdl-b* (Q) expressing nests in head-regenerating halves after 2 (L, left), 6 (Q, left), 20 (O, cryosection), 40 (M), 55 (N) h and basal regenerating halves after 2 (L, right), 6 (Q, right), (P, left) and 55 (P, right) h. Arrows indicate boundaries of the presumptive or newly formed apical region, arrowheads the presumptive or newly formed basal region. Scale bars: 400 μm in A–G, L, P; 300 μm in M, N; 200 μm in H–K, O, Q.

activity induced by retinoic acid (RA) in a heterologous context. We thus performed transactivation studies in mammalian cells transfected with a RARE-luc reporter plasmid, the AmphiRAR, AmphiRXR pSG5 expression plasmids (Escriva et al., 2002), and increasing amounts of pSG5-hyCOUP-chim2 in the presence of all-trans retinoic acid (10^{-8} M). AmphiCOUP was used as a control (Fig. 10B). These assays showed that hyCOUP-TF significantly repressed the activation (about 2-fold) produced by RAR:RXR in the presence of all-trans RA upon the RARE and this repression was clearly dose-dependent.

Discussion

The class II of nuclear receptors genes are well conserved from cnidarians to bilaterians

So far, NR genes were detected exclusively in metazoans and our previous phylogenetical analyses had shown that the diversification of the NR superfamily occurred in two waves of gene duplication. An early one corresponded to the progressive emergence of the six classes of receptors shared by bilaterians (Laudet, 1997; Laudet and Grone-

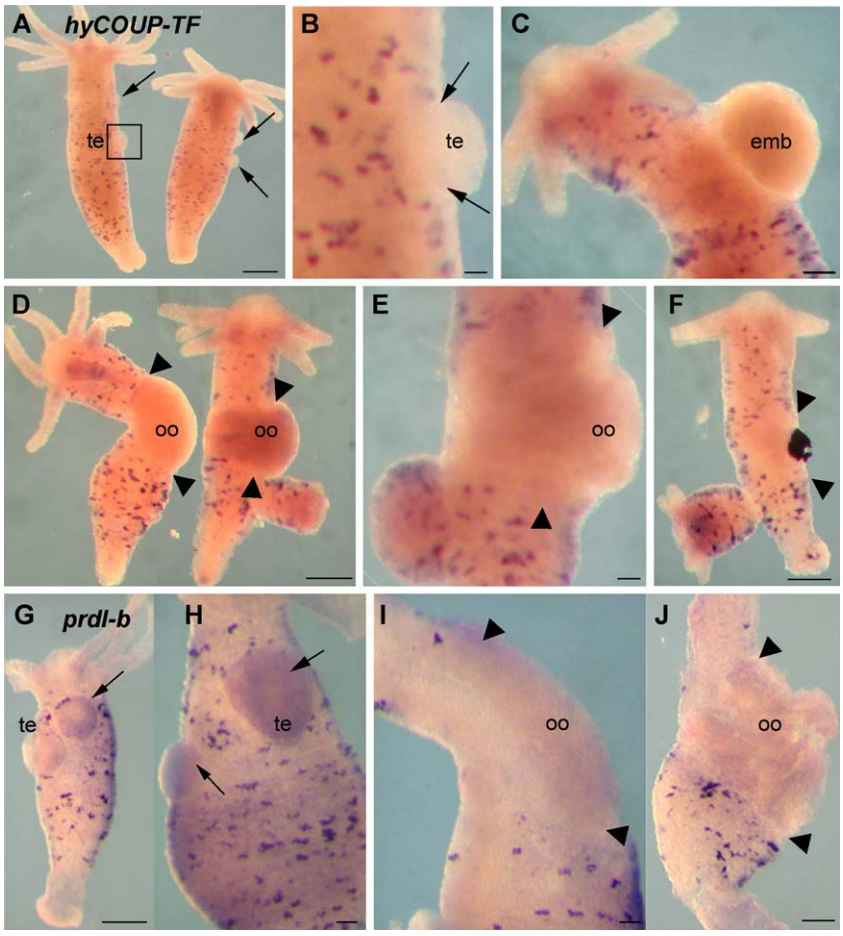

Fig. 9. Exclusion of *hyCOUP-TF* and *prdl-b* expressing cell clusters from regions undergoing spermatogenesis (A, B, G, H), ovogenesis (D, E, I, J), and early sexual development (C, F). Testes (te, arrows), in the upper half of the body column, show neither *hyCOUP-TF* (A, B) nor *prdl-b* (G, H) expression. Oocytes (oo, arowheads) develop on the whole circumference of the parent. In this belt, neither *hyCOUP-TF* (D, E) nor *prdl-b* (I, J) expressing cells were detected. At early stages when embryos (emb) develop on the parent, *hyCOUP-TF* expression was absent in the embryo but drastically reduced in the facing parental body column (C). After detachment of the embryo (F), *hyCOUP-TF* expression was progressively reestablished on the parental body column (arrowheads). The dark spot is a staining artifact corresponding to the area from which the embryo detached. Scale bars: 400 μm in A, D, F, G; 40 μm in B, C, E, H; 100 μm in I.

meyer, 2002) and a later one, vertebrate-specific, gave rise to the various paralogous copies of receptors such as COUP-TFI, COUP-TFII and EAR2 (Escriva et al., 1997, 2000). According to concordant phylogenetic analyses (Grasso et al., 2001), the hyCOUP-TF gene belongs to the monophyletic COUP family. The more divergent position of the hyCOUP-TF gene compared to that of the coral COUP homolog possibly suggests that the two genes are not orthologous, implying that other members of the COUP-TF group remain to be discovered in cnidarians. The fact that representatives of class II (COUP, RXR) and class V (FTZ-F1) NR superfamily were isolated in cnidarians (Escriva et al., 1997; Grasso et al., 2001; Kostrouch et al., 1998) supports the fact that the first wave of gene duplication occurred very early during metazoan evolution, predating the divergence between Cnidaria and Bilateria.

In vertebrates, *COUP-TFI* and *COUP-TFII* genes are splitted in three exons, separated by two introns, the first one being located at the junction between the C and D domains, and the second one in the E domain. Interestingly, the respective positions of these two introns are the two most conserved across the whole NR superfamily. The types II, III, and IV of *hyCOUP-TF* cDNAs isolated from hydra suggest that the first intron at the C/D domains boundary be conserved in cnidarians. So far, there are two examples of perfect conservation from hydra to vertebrates of intron position within regulatory genes: both were noted within regions encoding DNA-binding domains, one within the CREB gene (Galliot et al., 1995), the second within the *prdl-a* homeobox gene (Gauchat et al., 1998). In addition, hyCOUP-TF exhibits at least three distinct isoforms, differing by the presence of a deletion or an insertion within the D domain, implying a complex regulation of this gene at the post-transcriptional level. In *Drosophila*, the *COUP-TF* homolog, *svp*, is transcribed as two isoforms differing in their C-terminal part (Mlodzik et al., 1990).

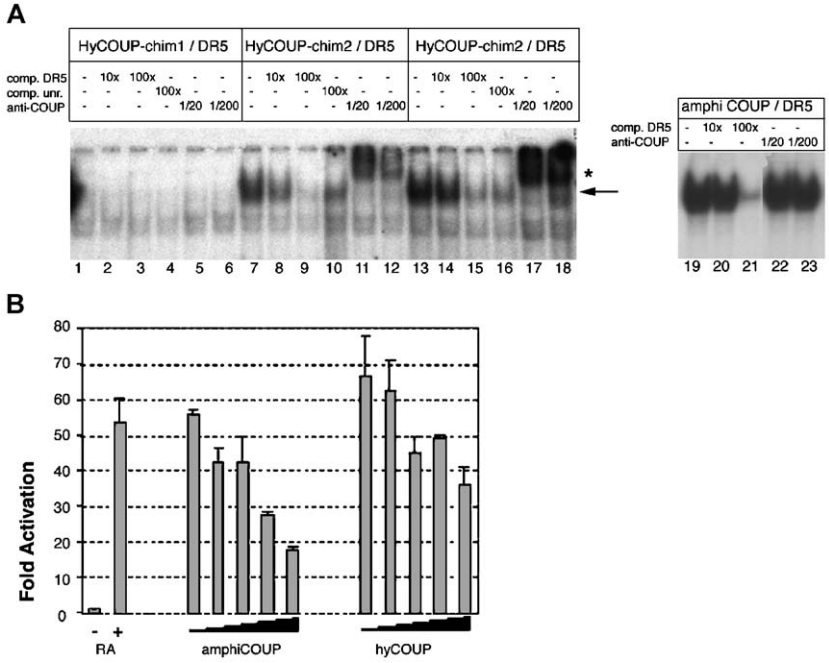

Fig. 10. DNA-binding and repressor activities of the HyCOUP-TF transcription factor. (A) DNA-binding activity of the hyCOUP-chim1 (lanes 1–6), hyCOUP-chim2 (lanes 7–18) and amphiCOUP (lanes 19–23) proteins were assayed onto the DR5 and DR1 response elements in gel retardation assays. Specific binding was not detected with hyCOUP-chim1, while hyCOUP-chim2 exhibited a specific binding on both DR5 (lanes 7–10) and DR1 (lanes 13–16), supershifted in the presence of the T19 antiserum (star, lanes 11, 12, 17, 18). AmphiCOUP specific binding onto DR5 was detected in the same experiment with a five times shorter exposure, but was not supershifted in the presence of T19 antiserum. (B) Transcriptional activities of the luciferase reporter construct pGL2-DR5-3× containing the DR5 consensus RA-responsive element. Values are averages of three independent transfection experiments carried out in Ros 17.2/8 cells and are depicted as fold activation relative to control values obtained in the same experiment, that is, AmphiRAR and AmphiRXR constructs expressed in the absence of all-trans-RA. The dose-dependent repression of transactivation induced by AmphiRAR:AmphiRXR after all-trans-RA treatment (10^{-8} M) on a DR5 element was observed when either AmphiCOUP-TF (10 to 500 ng) or hyCOUP-chim2 (100 to 1000 ng) were expressed. Error bars indicate standard deviations.

HyCOUP-TF and prdl-b appear as cell differentiation but not developmental genes in hydra

The *hyCOUP-TF* and *prdl-b* are both expressed in the nematocyte and the neuronal cell lineages as well as in a subset of interstitial stem cells, but were not detected during budding, regeneration, gametogenesis, and early sexual development. In the adult polyp, *hyCOUP-TF* and *prdl-b* genes exhibited an ectodermal "patchy" expression pattern, corresponding to cell clusters composed of small-sized, round cells, which according to their morphology, organization, location, and BrdU labeling index were characterized as dividing and differentiating nematoblasts, the precursor cells of mature nematocytes. In most cell clusters, *prdl-b* and *hyCOUP-TF* were found co-expressed while we recorded a clear restriction of their expression domains within the body column. It was actually demonstrated that nematocyte differentiation is inhibited in the head and basal regions (Fujisawa et al., 1986) and other gene markers for the nematocyte lineage display similar restriction of their expression patterns (Engel et al., 2002; Fedders et al., 2004; Gauchat et al., 1998; Grens et al., 1995; Lindgens et al., 2004). Cellular comparative analyses performed onto the *hyzic*, *CnASH* and *NOWA* expressing cells showed that *hyzic* is expressed quite early in the nematocyte pathway, predominantly in 4 and 8 cell clusters, very similarly to *prdl-b*, while *CnASH* and *Nowa* were expressed at later stages in 8 and 16 cell clusters (Lindgens et al., 2004). The BrdU labeling index of *hyzic* expressing cells measured after 1 h was already 40%, much higher than that measured for *prdl-b*, however, after 24 h, *hyzic* and *prdl-b* BrdU labeling indexes reach similar values (over 90% of the cells). This difference noted after a short incubation time, beside a difference in the starvation conditions, might indicate that *hyzic* and *prdl-b* are expressed in distinct subpopulations of the 2 cell clusters. The comparative analyses we performed on the distribution of nest sizes and the presence of differentiating capsules in expressing nests, in the BrdU labeling index of starving animals and during elimination of the interstitial cell lineage indicate that *hyCOUP-TF* and *prdl-b* likely play distinct roles in the control of the nematocyte pathway. Two major differences were recorded in the regulation of these two genes: first *prdl-b* expression is activated at least at two distinct stages of the nematocyte pathway but significantly in 2 cell clusters, while that of *hyCOUP-TF* is induced one run of division later, its expression being predominant at the 8 cells stage; second, *prdl-b* is expressed in proliferating nests while a significant subset of *hyCOUP-TF* expressing cell clusters are no longer cycling, escaping from proliferation to differentiate. Consequently, *hyCOUP-TF* might promote

entry into the differentiation process, while a possible function for *prdl-b* would rather be to keep the cells cycling. At differentiation stages, *hyCOUP-TF* expression did not seem to persist for long. However, the structural Nowa protein participates in nematocysts formation long after the *Nowa* gene expression is extinguished (Engel et al., 2002). Similarly, we cannot exclude that the hyCOUP-TF transcription factor be still active in mature nematocytes.

In most contexts COUP-TF transcription factors behave as potent negative transcriptional regulators (Achatz et al., 1997). We could detect a significant hyCOUP-TF transcriptional repressive activity in mammalian cells. The fact that hyCOUP-TF, when expressed in mammalian cells, represses the activation mediated by other NRs suggests that this activity is conserved in all metazoans. Thus, the regulatory function of COUP-TF on other members of the superfamily observed in vertebrates or *Drosophila* is not the by-product of a receptor that has lost its ligand but is a fundamental ancestral activity of this gene product. Hence, interacting NRs likely played key functions in the genetic cascades that regulated differentiation early in metazoan evolution, similarly to what was observed with the bHLH family members in myogenesis (Muller et al., 2003). Although hyCOUP-TF transcriptional activity remains to be tested in hydra interstitial cells, this repressive activity might be required in nematoblasts to direct the transition from proliferation to differentiation stages. For example, a direct regulation of the hyCOUP-TF transcription factor upon the *prdl-b* gene can be envisaged similarly to the mouse *Mix* paired-like gene that displays COUP-TF binding sites in its promoter (Sahr et al., 2002).

Highly evolutionarily conserved regulatory genes as COUP-TF and paired-like genes trace back to the early steps of neurogenesis

In vertebrates, COUP-TFI disruption results in multiple defects of the central nervous system (Qiu et al., 1997). In mouse embryos, null mutation of mCOUP-TFI induces defects in glossopharyngeal ganglion and abnormal axonal projections are observed in several regions. COUP-TFI is involved in the segmentation of the diencephalon (Qiu et al., 1994) and is an early intrinsic factor for early regionalization of the neocortex (Zhou et al., 2001). In contrast, the COUP-TFII gene seems to be devoted to mesenchymal–epithelial interactions during organogenesis (Pereira et al., 1999). The counterpart of COUP-TF genes in *Drosophila*, Seven-up (svp) is implicated in photoreceptor determination (Mlodzik et al., 1990). Finally, in amphioxus, the *COUP-TF* gene is expressed in the nerve cord of late larvae (Langlois et al., 2000). Altogether, these data show that *COUP-TF*-related genes are implicated both in neurogenesis and/or CNS patterning during the embryonic life of a evolutionarily distant species.

Similarly, in hydra *hyCOUP-TF* is expressed in two lineages that define the rudimentary nervous system of cnidarians, mechanoreceptor cells, and neuronal cells, and is thus likely involved in neurogenesis. Interestingly, *hyCOUP-TF* and *prdl-b* are two evolutionarily conserved regulatory genes that are expressed in two cell lineages, which derive from a common stock of interstitial stem cells. We recently observed that the ParaHox *Gsx*-related *cnox-2* gene (Gauchat et al., 2000) also displays this dual expression (M.M-L, unpublished). This "comparative molecular cell biology approach" implies that cells from the nematocyte and the neuronal cell lineages can be considered as "sister cell types that evolved from a common precursor by cell type diversification" (Arendt, 2003), suggesting that a yet unidentified fraction of interstitial cells are specific precursors for the nematocyte and neuronal cell lineages. We would expect that *hyCOUP-TF*, *prdl-b*, and *cnox-2* are markers of this common precursor.

We previously showed that the paired-like gene *prdl-a* is expressed in the neuronal cell lineage in hydra (Gauchat et al., 1998), the paired-like genes being mostly devoted to neurogenesis in Bilateria. Therefore, we assume that neurogenesis corresponded to the ancestral cellular function of both *COUP-TF* and paired-like genes, similarly to what was proposed for the *hyzic* genes (Lindgens et al., 2004) and that neurogenesis evolved only once (Galliot and Miller, 2000). According to the most parsimonious scenario (Miljkovic-Licina et al., in press), a common ancestor to cnidarians and bilaterians would have differentiated "proto-neuronal" cells, possibly similar to mechanoreceptor cells, under the control of regulatory genes like *COUP-TF*, *paired-like* and *hyzic* genes, whose function in neurogenesis remained conserved in most phyla.

Acknowledgments

We thank Sabina Hoffmeister, Dick Campbell, Thomas Bosch, Andreas Fröbius and Thomas Holstein for sending us various hydra strains, Chica Schaller and Hans Bode for their generous gifts of hydra cDNA libraries, Z. Kostrouch and J. Rall for the *Tripedalia* RXR clone, Daniel Roppolo and Yvan Rodriguez for helping us with the double in situ procedure, Volker Schmid for stimulating discussions. This work was supported by the Swiss National Foundation (FNS 31-59462.99), the Canton of Geneva, the Fonds Georges et Antoine Claraz, the Academic Society of Geneva, the Association in favor of the Cancer Research, the CNRS, the French National Education, Research and Technology Ministry and the Rhone-Alp District.

Appendix A. Supplementary data

Supplementary data associated with this article can be found, in the online version, at doi:10.1016/j.ydbio.2004.07.037.

References

Achatz, G., Holzl, B., Speckmayer, R., Hauser, C., Sandhofer, F., Paulweber, B., 1997. Functional domains of the human orphan receptor ARP-1/COUP-TFII involved in active repression and transrepression. Mol. Cell. Biol. 17, 4914–4932.

Aerne, B.L., Stidwill, R.P., Tardent, P., 1991. Nematocyte discharge in hydra does not require the presence of nerve cells. J. Exp. Zool. 258, 137–141.

Anderson, P.A.V., 1990. Evolution of the First Nervous Systems. Plenum Press, New York.

Arendt, D., 2003. Evolution of eyes and photoreceptor cell types. Int. J. Dev. Biol. 47, 563–571.

Bode, H.R., 1996. The interstitial cell lineage of hydra: a stem cell system that arose early in evolution. J. Cell Sci. 109, 1155–1164.

Bosch, T.C., David, C.N., 1984. Growth regulation in hydra: relationship between epithelial cell cycle length and growth rate. Dev. Biol. 104, 161–171.

Bourguet, W., Ruff, M., Chambon, P., Gronemeyer, H., Moras, D., 1995. Crystal structure of the ligand-binding domain of the human nuclear receptor RXR-alpha. Nature 375, 377–382.

Campbell, R.D., Marcum, B.A., 1980. Nematocyte migration in hydra: evidence for contact guidance in vivo. J. Cell Sci. 41, 33–51.

Cikala, M., Wilm, B., Hobmayer, E., Bottger, A., David, C.N., 1999. Identification of caspases and apoptosis in the simple metazoan hydra. Curr. Biol. 9, 959–962.

Cooney, A.J., Lee, C.T., Lin, S.C., Tsai, S.Y., Tsai, M.J., 2001. Physiological function of the orphans GCNF and COUP-TF. Trends Endocrinol. Metab. 12, 247–251.

David, C.N., 1973. A quantitative method for maceration of hydra tissue. Wilhelm Roux' Arch. Dev. Biol. 171, 259–268.

Dayhoff, M.O., Schwartz, R.M., Orcutt, B.C., 1978. A Model of Evolutionary Change in Proteins. National Biomedical Research Foundation, Washington, DC.

Devine, C., Hinman, V.F., Degnan, B.M., 2002. Evolution and developmental expression of nuclear receptor genes in the ascidian herdmania. Int. J. Dev. Biol. 46, 687–692.

Duarte, J., Perriere, G., Laudet, V., Robinson-Rechavi, M., 2002. NUREBASE: database of nuclear hormone receptors. Nucleic Acids Res. 30, 364–368.

Engel, U., Oezbek, S., Engel, R., Petri, B., Lottspeich, F., Holstein, T.W., 2002. Nowa, a novel protein with minicollagen cys-rich domains, is involved in nematocyst formation in hydra. J. Cell Sci. 115, 3923–3934.

Escriva, H., Safi, R., Hanni, C., Langlois, M.C., Saumitou-Laprade, P., Stehelin, D., Capron, A., Pierce, R., Laudet, V., 1997. Ligand binding was acquired during evolution of nuclear receptors. Proc. Natl. Acad. Sci. U. S. A. 94, 6803–6808.

Escriva, H., Delaunay, F., Laudet, V., 2000. Ligand binding and nuclear receptor evolution. BioEssays 22, 717–727.

Escriva, H., Holland, N.D., Gronemeyer, H., Laudet, V., Holland, L.Z., 2002. The retinoic acid signaling pathway regulates anterior/posterior patterning in the nerve cord and pharynx of amphioxus, a chordate lacking neural crest. Development 129, 2905–2916.

Fedders, H., Augustin, R., Bosch, T.C., 2004. A Dickkopf- 3-related gene is expressed in differentiating nematocytes in the basal metazoan hydra. Dev. Genes Evol. 214, 72–80.

Fujisawa, T., David, C.N., 1984. Loss of differentiating nematocytes induced by regeneration and wound healing in hydra. J. Cell Sci. 68, 243–255.

Fujisawa, T., Nishimiya, C., Sugiyama, T., 1986. Nematocyte differentiation in hydra. Curr. Top. Dev. Biol. 20, 281–290.

Galliot, B., Miller, D., 2000. Origin of anterior patterning. How old is our head? Trends Genet. 16, 1–5.

Galliot, B., Welschof, M., Schuckert, O., Hoffmeister, S., Schaller, H.C., 1995. The cAMP response element binding protein is involved in hydra regeneration. Development 121, 1205–1216.

Galliot, B., de Vargas, C., Miller, D., 1999. Evolution of homeobox genes: Q50 paired-like genes founded the paired class. Dev. Genes Evol. 209, 186–197.

Gauchat, D., Kreger, S., Holstein, T., Galliot, B., 1998. prdl-a, a gene marker for hydra apical differentiation related to triploblastic paired-like head-specific genes. Development 125, 1637–1645.

Gauchat, D., Mazet, F., Berney, C., Schummer, M., Kreger, S., Pawlowski, J., Galliot, B., 2000. Evolution of Antp-class genes and differential expression of hydra Hox/paraHox genes in anterior patterning. Proc. Natl. Acad. Sci. U. S. A. 97, 4493–4498.

Giguere, V., 1999. Orphan nuclear receptors: from gene to function. Endocr. Rev. 20, 689–725.

Grasso, L.C., Hayward, D.C., Trueman, J.W., Hardie, K.M., Janssens, P.A., Ball, E.E., 2001. The evolution of nuclear receptors: evidence from the coral Acropora. Mol. Phylogenet. Evol. 21, 93–102.

Grens, A., Mason, E., Marsh, J.L., Bode, H.R., 1995. Evolutionary conservation of a cell fate specification gene: the hydra achaete–scute homolog has proneural activity in *Drosophila*. Development 121, 4027–4035.

Grens, A., Gee, L., Fisher, D.A., Bode, H.R., 1996. CnNK-2, an NK-2 homeobox gene, has a role in patterning the basal end of the axis in hydra. Dev. Biol. 180, 473–488.

Holmbeck, S.M., Foster, M.P., Casimiro, D.R., Sem, D.S., Dyson, H.J., Wright, P.E., 1998. High-resolution solution structure of the retinoid X receptor DNA-binding domain. J. Mol. Biol. 281, 271–284.

Holstein, T.W., David, C.N., 1990. Cell cycle length, cell size, and proliferation rate in hydra stem cells. Dev. Biol. 142, 392–400.

Holstein, T., Emschermann, P., 1995. Zytologie. In: Schwoerbel, J., Zwick, P. Cnidaria: Hydrozoa, Kamptozoa (Eds.), vol. 1. Gustav Fisher Verlag, Stuttgart, pp. 5–15.

Holstein, T., Hausmann, K., 1988. The cnidocil apparatus of hydrozoans: a progenitor of metazoan mechanoreceptors? In: Hessinger, D.A., Lenhoff, H.M. (Eds.), The Biology of Nematocysts. Academic Press, San Diego, pp. 53–73.

Holstein, T., Tardent, P., 1984. An ultrahigh-speed analysis of exocytosis: nematocyst discharge. Science 223, 830–833.

Holstein, T.W., Hobmayer, E., David, C.N., 1991. Pattern of epithelial cell cycling in hydra. Dev. Biol. 148, 602–611.

Holstein, T.W., Hobmayer, E., Technau, U., 2003. Cnidarians: an evolutionarily conserved model system for regeneration? Dev. Dyn. 226, 257–267.

Holtmann, M., Thurm, U., 2001a. Mono- and oligo-vesicular synapses and their connectivity in a Cnidarian sensory epithelium (*Coryne tubulosa*). J. Comp. Neurol. 432, 537–549.

Holtmann, M., Thurm, U., 2001b. Variations of concentric hair cells in a Cnidarian sensory epithelium (Coryne tubulosa). J. Comp. Neurol. 432, 550–563.

Kass-Simon, G., Scappaticci, A.A., 2002. The behavioral and developmental physiology of nematocysts. Can. J. Zool. 80, 1772–1794.

Kostrouch, Z., Kostrouchova, M., Love, W., Jannini, E., Piatigorsky, J., Rall, J.E., 1998. Retinoic acid X receptor in the diploblast, *Tripedalia cystophora*. Proc. Natl. Acad. Sci. U. S. A. 95, 13442–13447.

Langlois, M.C., Vanacker, J.M., Holland, N.D., Escriva, H., Queva, C., Laudet, V., Holland, L.Z., 2000. Amphicoup-TF, a nuclear orphan receptor of the lancelet *Branchiostoma floridae*, is implicated in retinoic acid signalling pathways. Dev. Genes Evol. 210, 471–482.

Larsen, N., Olsen, G.J., Maidak, B.L., McCaughey, M.J., Overbeek, R., Macke, T.J., Marsh, T.L., Woese, C.R., 1993. The ribosomal database project. Nucleic Acids Res. 21, 3021–3023.

Laudet, V., 1997. Evolution of the nuclear receptor superfamily: early diversification from an ancestral orphan receptor. J. Mol. Endocrinol. 19, 207–226.

Laudet, V., Gronemeyer, H., 2002. The Nuclear Receptors. Academic Press.

Lehn, H., 1951. Teilungsfolden und Determination von I-zellen fuer die Cnidenbildung bei Hydra. Zoologische Naturforschung, B 6, 388–391.

Lindgens, D., Holstein, T.W., Technau, U., 2004. Hyzic, the hydra homolog

of the zic/odd-paired gene, is involved in the early specification of the sensory nematocytes. Development 131, 191–201.
Mackie, G.O., 1990. The elementary nervous system revisited. Am. Zool. 30, 907–920.
Marcum, B.A., Fujisawa, T., Sugiyama, T., 1980. A mutant hydra strain (sf-1) containing temperature-sensitive interstitial cells. In: Tardent, P., Tardent, R. (Eds.), Developmental and Cellular Biology of Coelenterates. Elsevier/North Holland, Amsterdam, pp. 429–434.
Martin, V.J., Littlefield, C.L., Archer, W.E., Bode, H.R., 1997. Embryogenesis in hydra. Biol. Bull. 192, 345–363.
Miljkovic-Licina, M., Gauchat, D., Galliot, B., 2004. Neuronal evolution: analysis of regulatory genes in a first-evolved nervous system, the hydra nervous system. BioSystems (in press).
Mlodzik, M., Hiromi, Y., Weber, U., Goodman, C.S., Rubin, G.M., 1990. The *Drosophila* seven-up gene, a member of the steroid receptor gene superfamily, controls photoreceptor cell fates. Cell 60, 211–224.
Moras, D., Gronemeyer, H., 1998. The nuclear receptor ligand-binding domain: structure and function. Curr. Opin. Cell Biol. 10, 384–391.
Muller, P., Seipel, K., Yanze, N., Reber-Muller, S., Streitwolf-Engel, R., Stierwald, M., Spring, J.J., Schmid, V., 2003. Evolutionary aspects of developmentally regulated helix–loop–helix transcription factors in striated muscle of jellyfish. Dev. Biol. 255, 216–229.
Nuclear Receptor Nomenclature Committee, 1999. A unified nomenclature system for the nuclear receptor superfamily. Cell 97, 161–163.
Otto, J.J., Campbell, R.D., 1977. Budding in Hydra attenuata: bud stages and fate map. J. Exp. Zool. 200, 417–428.
Pereira, F.A., Qiu, Y., Zhou, G., Tsai, M.J., Tsai, S.Y., 1999. The orphan nuclear receptor COUP-TFII is required for angiogenesis and heart development. Genes Dev. 13, 1037–1049.
Pereira, F.A., Tsai, M.J., Tsai, S.Y., 2000. COUP-TF orphan nuclear receptors in development and differentiation. Cell. Mol. Life Sci. 57, 1388–1398.
Qiu, Y., Cooney, A.J., Kuratani, S., DeMayo, F.J., Tsai, S.Y., Tsai, M.J., 1994. Spatiotemporal expression patterns of chicken ovalbumin upstream promoter-transcription factors in the developing mouse central nervous system: evidence for a role in segmental patterning of the diencephalon. Proc. Natl. Acad. Sci. U. S. A. 91, 4451–4455.
Qiu, Y., Pereira, F.A., DeMayo, F.J., Lydon, J.P., Tsai, S.Y., Tsai, M.J., 1997. Null mutation of mCOUP-TFI results in defects in morphogenesis of the glossopharyngeal ganglion, axonal projection, and arborization. Genes Dev. 11, 1925–1937.
Renaud, J.P., Rochel, N., Ruff, M., Vivat, V., Chambon, P., Gronemeyer, H., Moras, D., 1995. Crystal structure of the RAR-gamma ligand-binding domain bound to all-trans retinoic acid. Nature 378, 681–689.
Rich, F., Tardent, P., 1969. Studies of differentiation of nematocytes in Hydra attenuata Pall. Rev. Suisse Zool. 76, 779–787.
Sahr, K., Dias, D.C., Sanchez, R., Chen, D., Chen, S.W., Gudas, L.J., Baron, M.H., 2002. Structure, upstream promoter region, and functional domains of a mouse and human Mix paired-like homeobox gene. Gene 291, 135–147.
Saitou, N., Nei, M., 1987. The neighbor-joining method: a new method for reconstructing phylogenetic trees. Mol. Biol. Evol. 4, 406–425.
Schaller, H.C., Hoffmeister, S.A., Dubel, S., 1989. Role of the neuropeptide head activator for growth and development in hydra and mammals. Development 107, 99–107.
Tardent, P., 1995. The cnidarian cnidocyte, a high-tech cellular weaponry. BioEssays 17, 351–362.
Terada, H., Sugiyama, T., Shigenaka, Y., 1988. Genetic analysis of developmental mechanisms in hydra: XVIII. Mechanism for elimination of the interstitial cell lineage in the mutant strain Sf-1. Dev. Biol. 126, 263–269.
Tsai, S.Y., Tsai, M.J., 1997. Chick ovalbumin upstream promoter-transcription factors (COUP-TFs): coming of age. Endocr. Rev. 18, 229–240.
Weber, G., Honegger, T., Tardent, P., 1978. Neuorientierung der Nesselzellwanderung bei Hydra attenuata Pall. Durch transplantierte Tentakel. Rev. Suisse Zool. 85, 768–774.
Westfall, J.A., 1996. Ultrastructure of synapses in the first-evolved nervous systems. J. Neurocytol. 25, 735–746.
Westfall, J.A., Elliott, C.F., Carlin, R.W., 2002. Ultrastructural evidence for two-cell and three-cell neural pathways in the tentacle epidermis of the sea anemone *Aiptasia pallida*. J. Morphol. 251, 83–92.
Wurtz, J.M., Bourguet, W., Renaud, J.P., Vivat, V., Chambon, P., Moras, D., Gronemeyer, H., 1996. A canonical structure for the ligand-binding domain of nuclear receptors. Nat. Struct. Biol. 3, 87–94.
Yaross, M.S., Bode, H.R., 1978. Regulation of interstitial cell differentiation in hydra attenuata: V. Inability of regenerating head to support nematocyte differentiation. J. Cell Sci. 34, 39–52.
Yon, J., Fried, M., 1989. Precise gene fusion by PCR. Nucleic Acids Res. 17, 4895.
Zhao, Q., Chasse, S.A., Devarakonda, S., Sierk, M.L., Ahvazi, B., Rastinejad, F., 2000. Structural basis of RXR–DNA interactions. J. Mol. Biol. 296, 509–520.
Zhou, C., Tsai, S.Y., Tsai, M.J., 2001. COUP-TFI: an intrinsic factor for early regionalization of the neocortex. Genes Dev. 15, 2054–2059.